# rigorous resonance determination ?

Jozef Dudek

hadspec
hadron spectrum collaboration
hadspec.org

William & Mary
CHARTERED 1693

Jefferson Lab
Thomas Jefferson National Accelerator Facility

# singularities in the complex energy plane



scattering amplitudes are measured for real energies above threshold

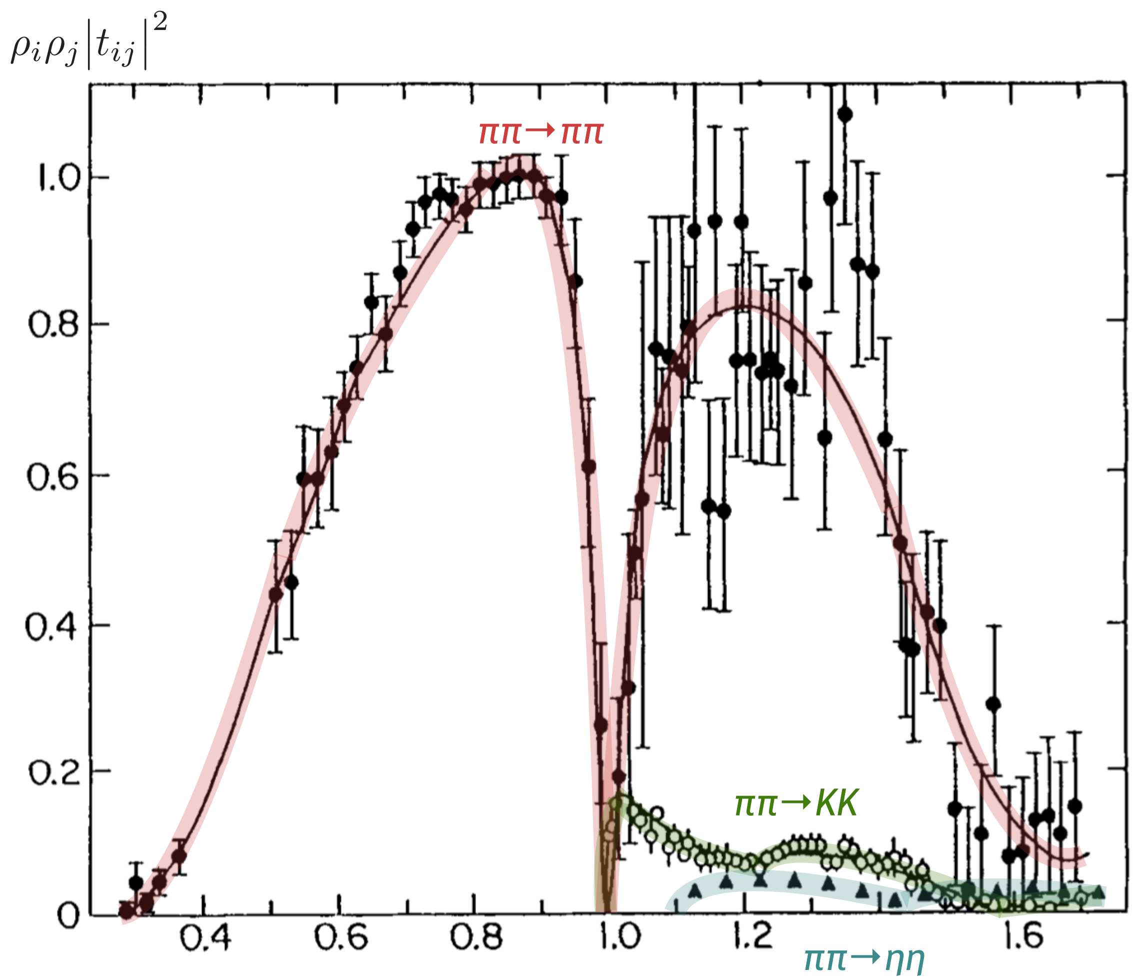



and we've seen that lattice calculations can lead to something similar

# singularities in the complex energy plane

does it make sense to consider how the amplitude behaves 'elsewhere'
— below threshold ?
— for complex values of $E$ ?

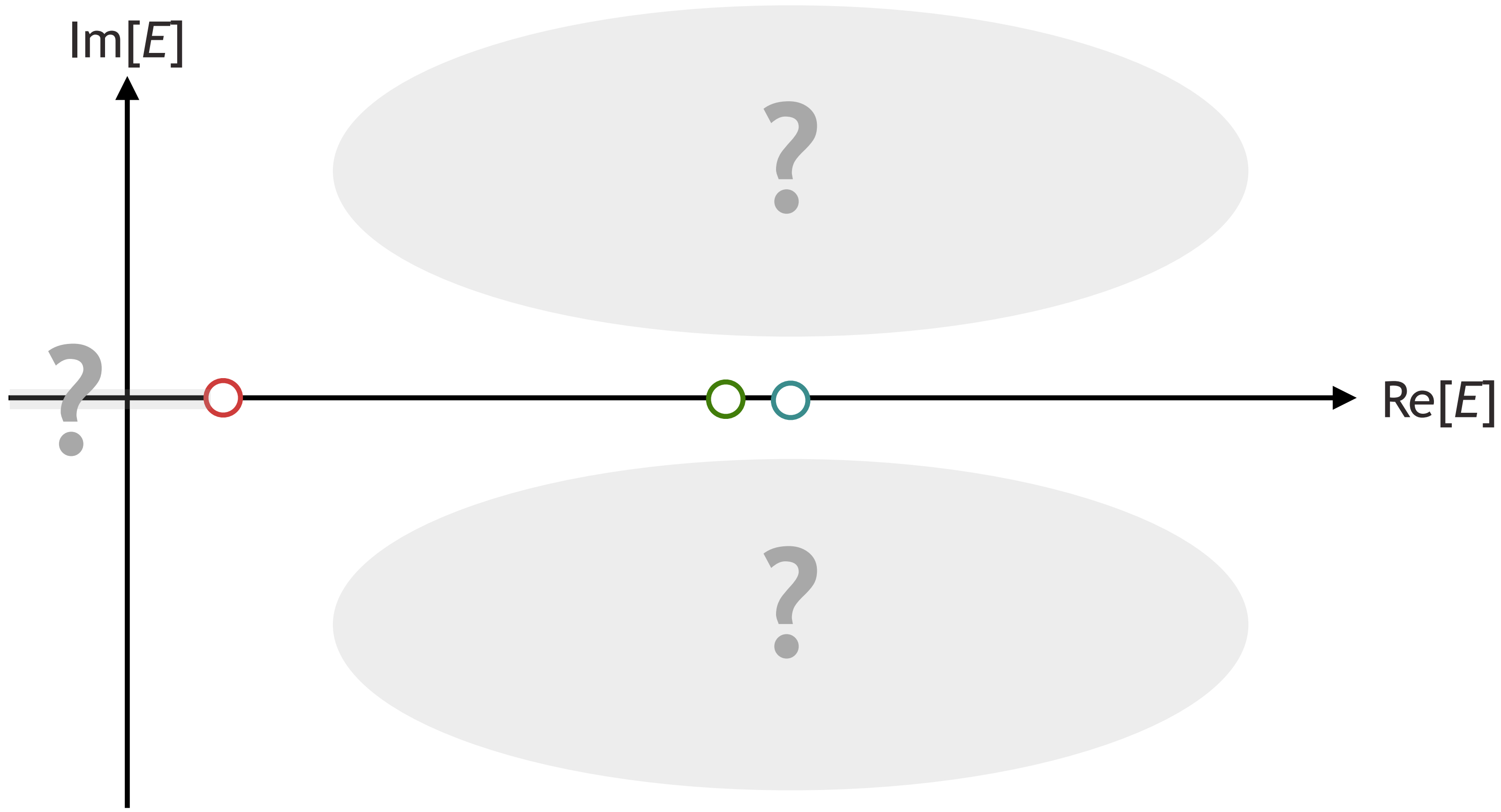


complex variable theory tells us that
**singularities (poles, cuts)**
control the behaviour of functions

— what singularities can our amplitudes have ?

# the unitarity cut

unitarity gives us one guaranteed singularity — a branch cut starting at threshold

e.g. elastic partial-wave case: $\mathrm{Im}\, t_\ell(s) = \rho(s)\,\big|t_\ell(s)\big|^2\,\Theta(s-4m^2)$

$$\rho(s) = \frac{2k(s)}{\sqrt{s}} = \frac{\sqrt{s-4m^2}}{\sqrt{s}}$$

square root branch cut

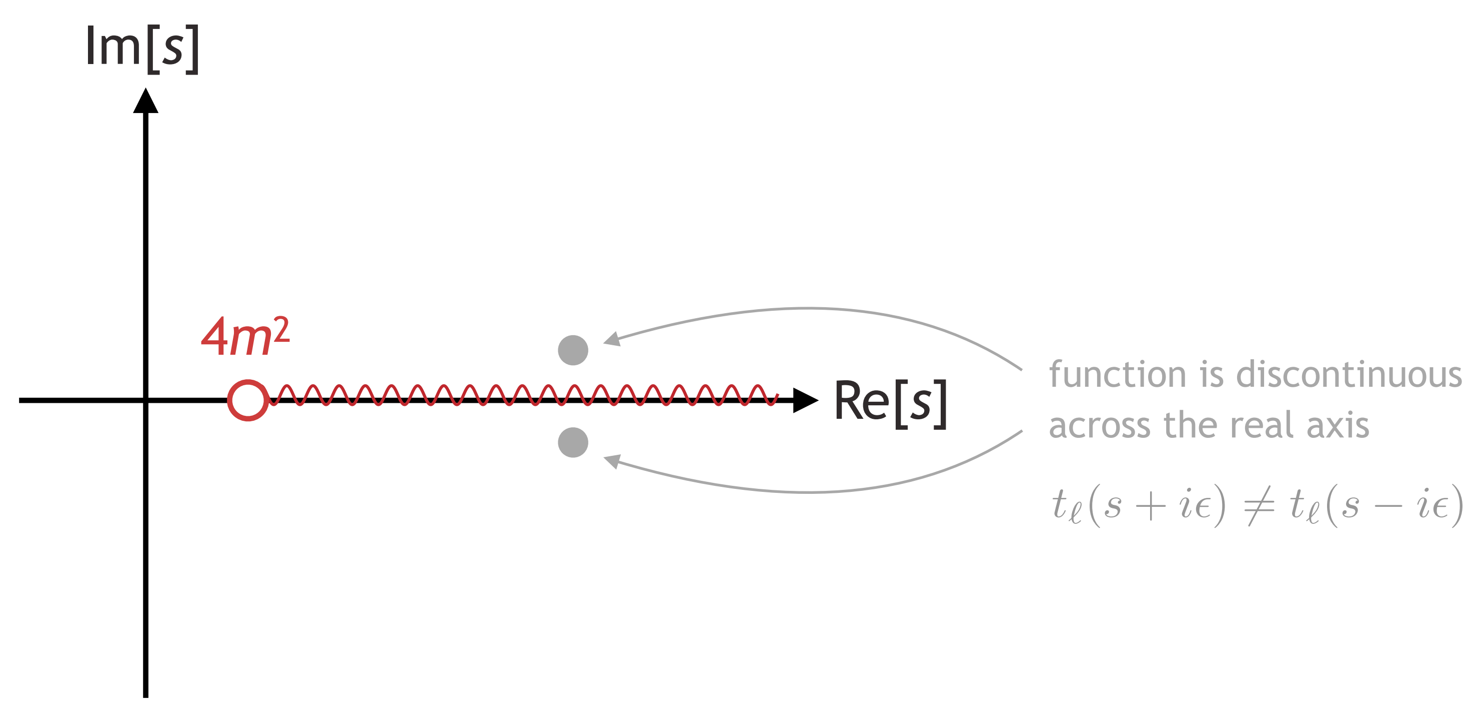


has an immediate consequence
— the complex plane must be **multi-sheeted**

# Riemann sheet structure

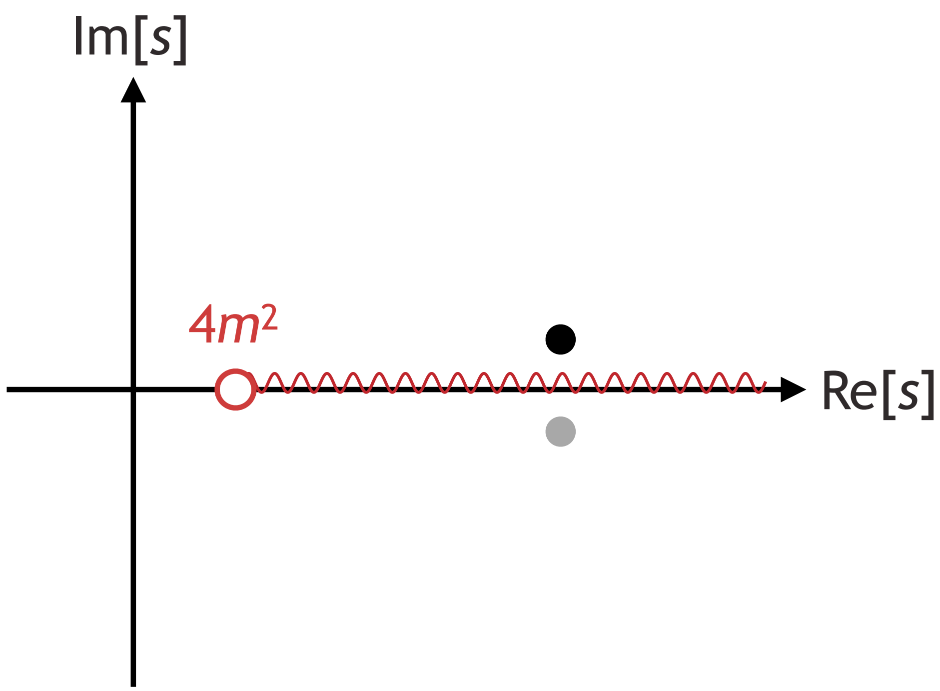


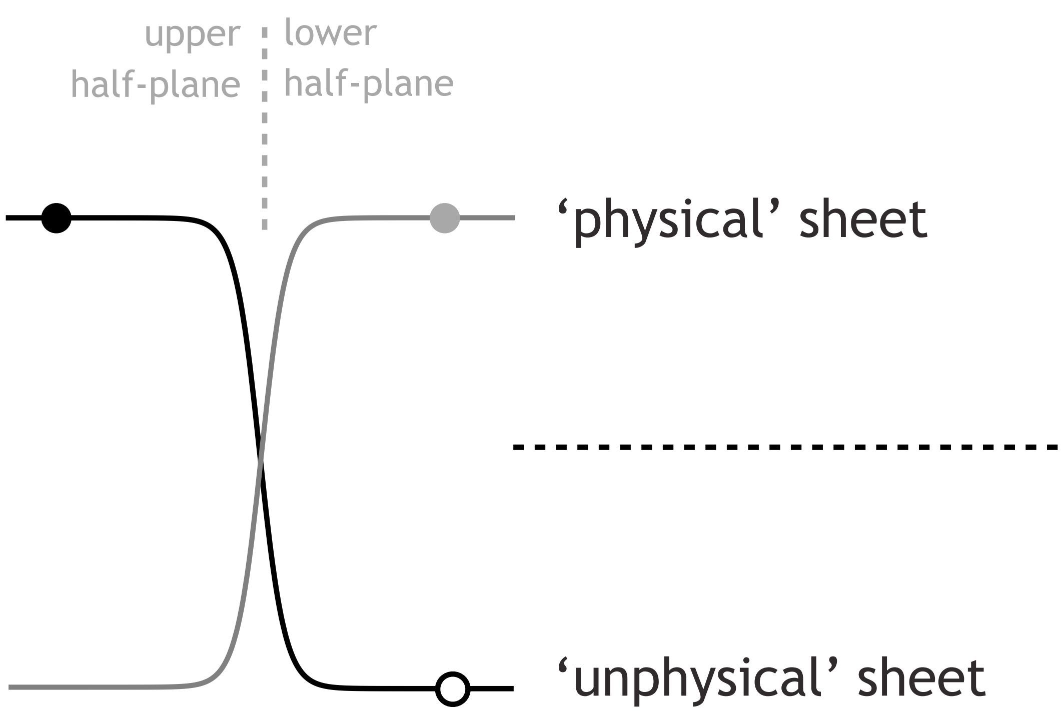


sheets can be characterised by the sign of Im[$k$]

physical sheet = sheet I = Im[$k$] > 0

unphysical sheet = sheet II = Im[$k$] < 0

# pole singularities ?



scattering amplitudes can have pole singularities only in certain locations

real energy axis, below threshold on **physical sheet**

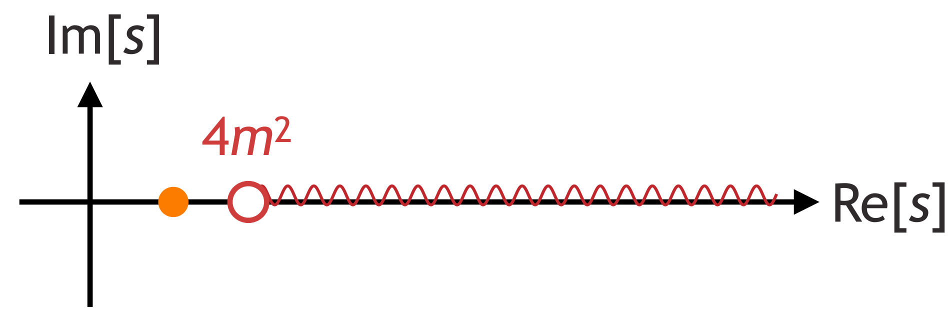


corresponds to a **stable bound-state**

off the real axis, on the **unphysical sheet**

(in complex conjugate pairs)

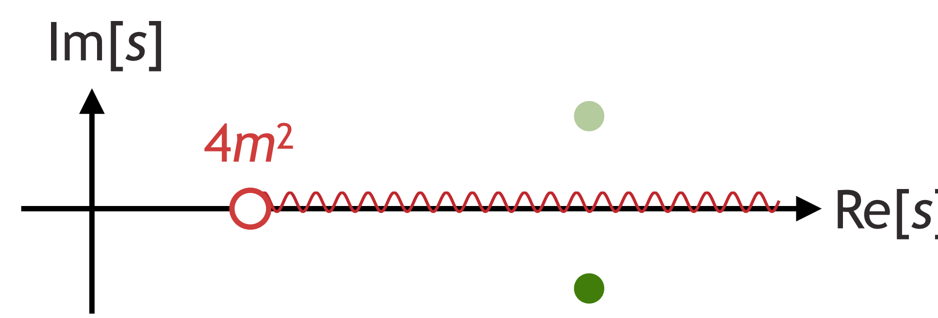


corresponds to a **resonance**

real energy axis, below threshold on **unphysical sheet**

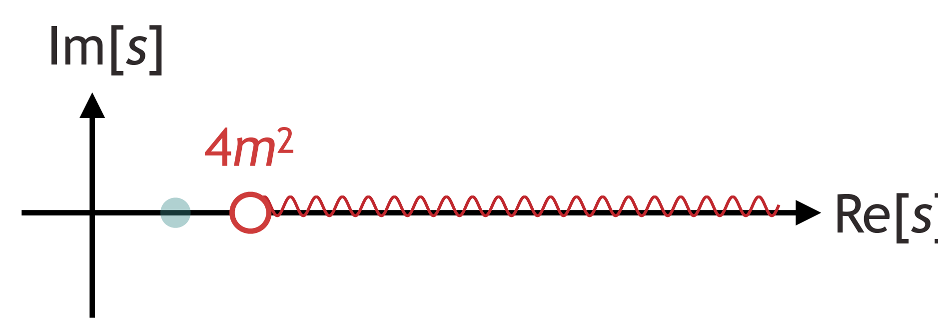


corresponds to a **virtual bound-state**

# pole singularities ?

scattering amplitudes can have pole singularities only in certain locations

**not allowed:** poles off the real axis
on the **physical sheet**

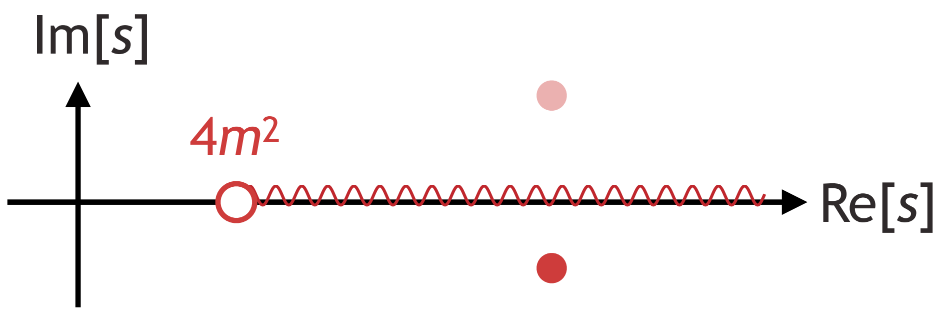


would violate **causality**

# a bound-state pole



will strongly enhance scattering at threshold

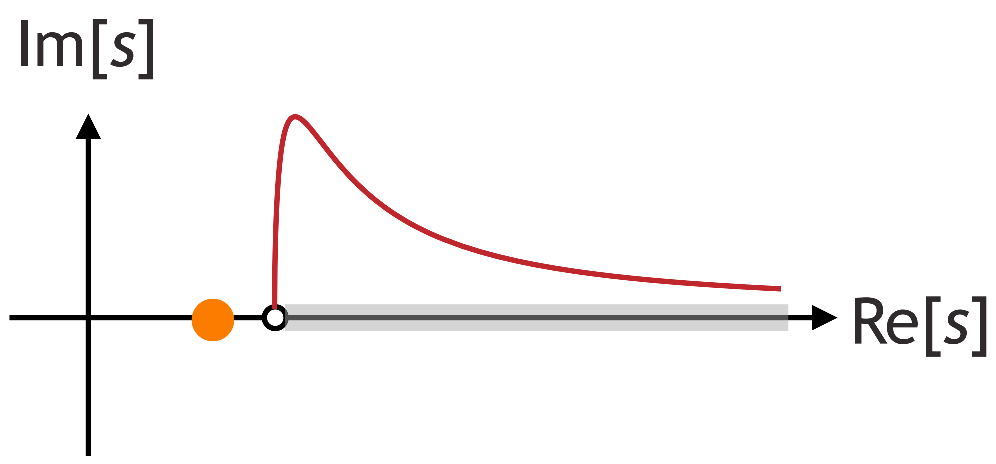


famous example is the deuteron at *NN* threshold

# pole on the unphysical sheet



an **isolated** pole on the unphysical sheet will produce a bump on the real axis

— the classic resonance signature

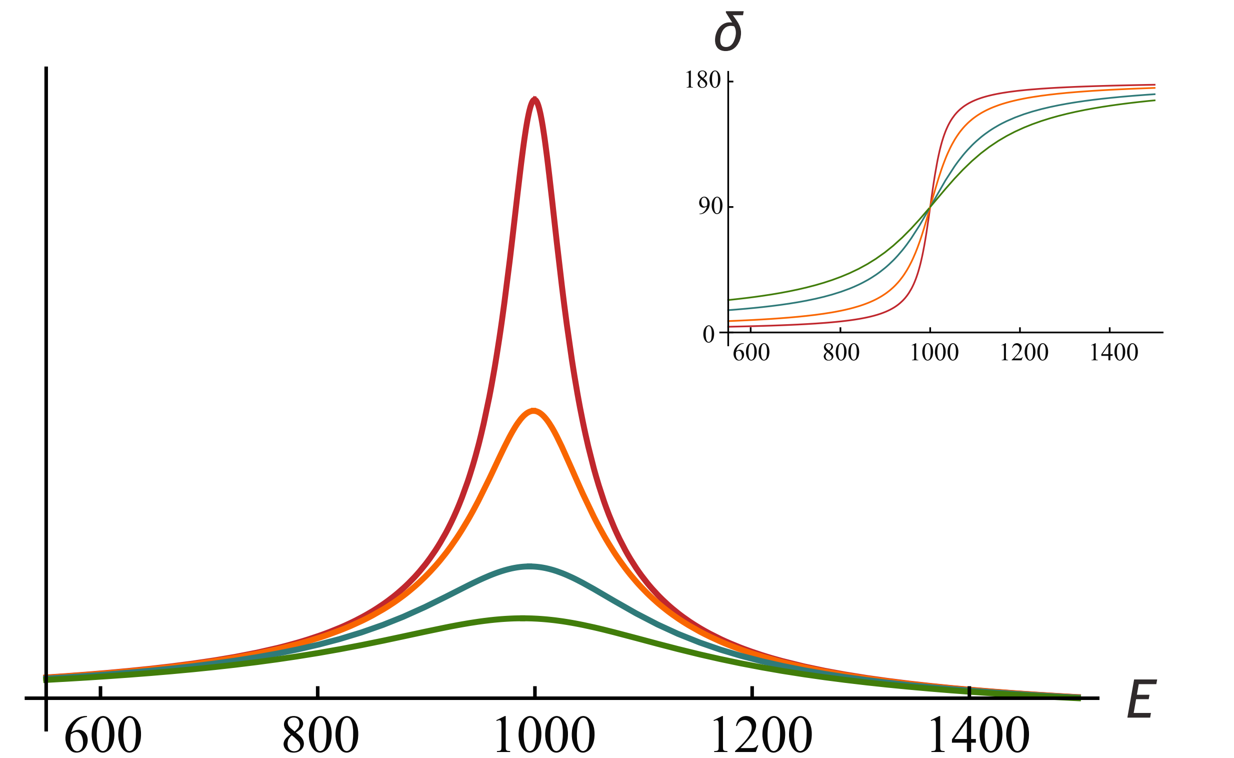


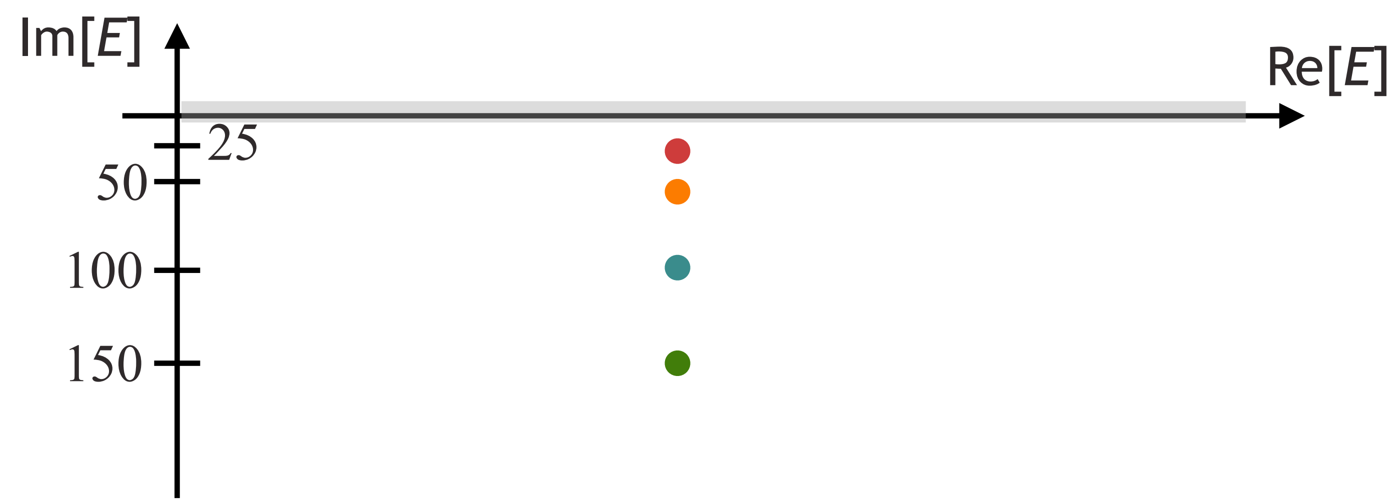


close to the pole

$$t_\ell(s) \sim \frac{1}{s_0 - s}$$

$$s_0 = \left(m - i\tfrac{1}{2}\Gamma\right)^2$$

# singularity structure from lattice calculations — elastic

$\pi\pi$ isospin=2

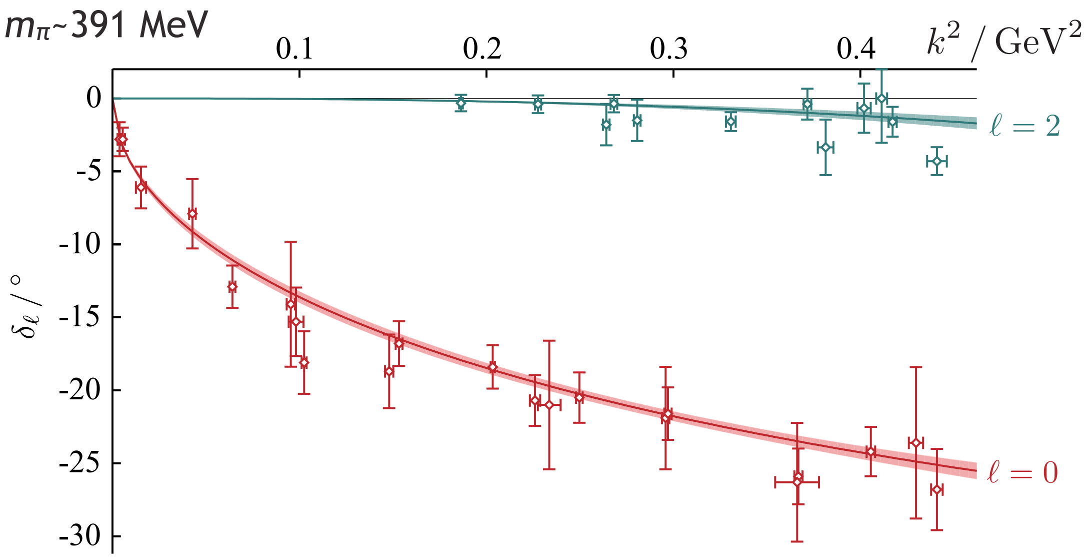


PRD86 034031 (2012)

**no nearby poles**

weak and repulsive interaction

$$k \cot \delta_0 = \frac{1}{a_0} + \ldots$$

$$m_\pi a_0 = -0.285(6)$$

$$s_0 \approx -45\, m_\pi^2$$

# singularity structure from lattice calculations — elastic

## $\pi\pi$ isospin=1

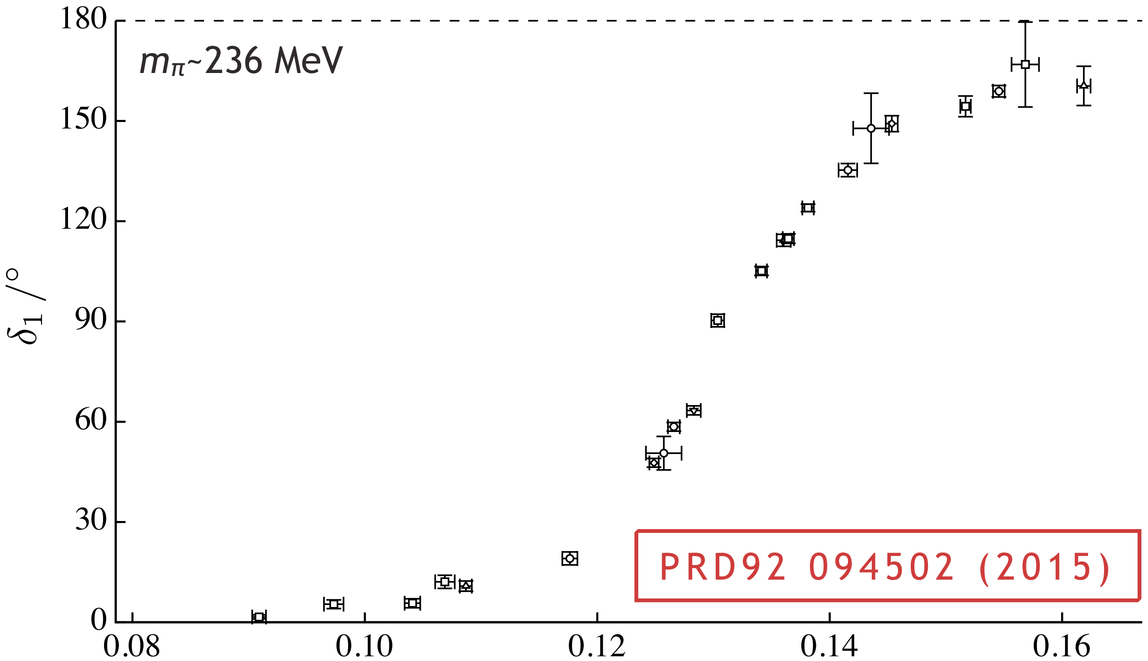


PRD92 094502 (2015)

**a single isolated pole**

a narrow resonance

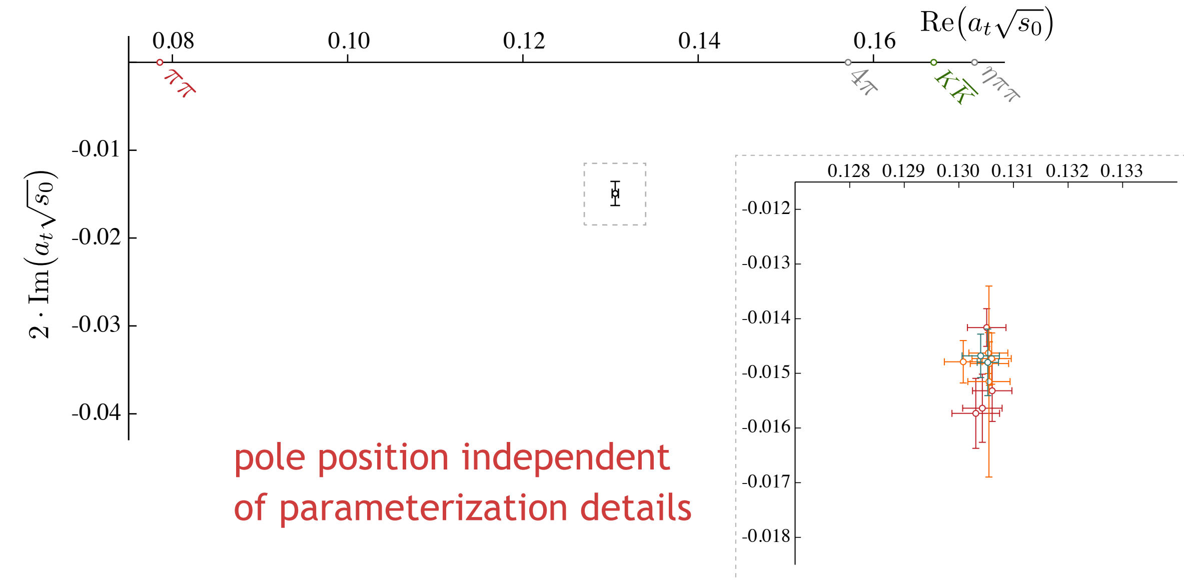


pole position independent of parameterization details

# singularity structure from lattice calculations — elastic

## ππ isospin=1

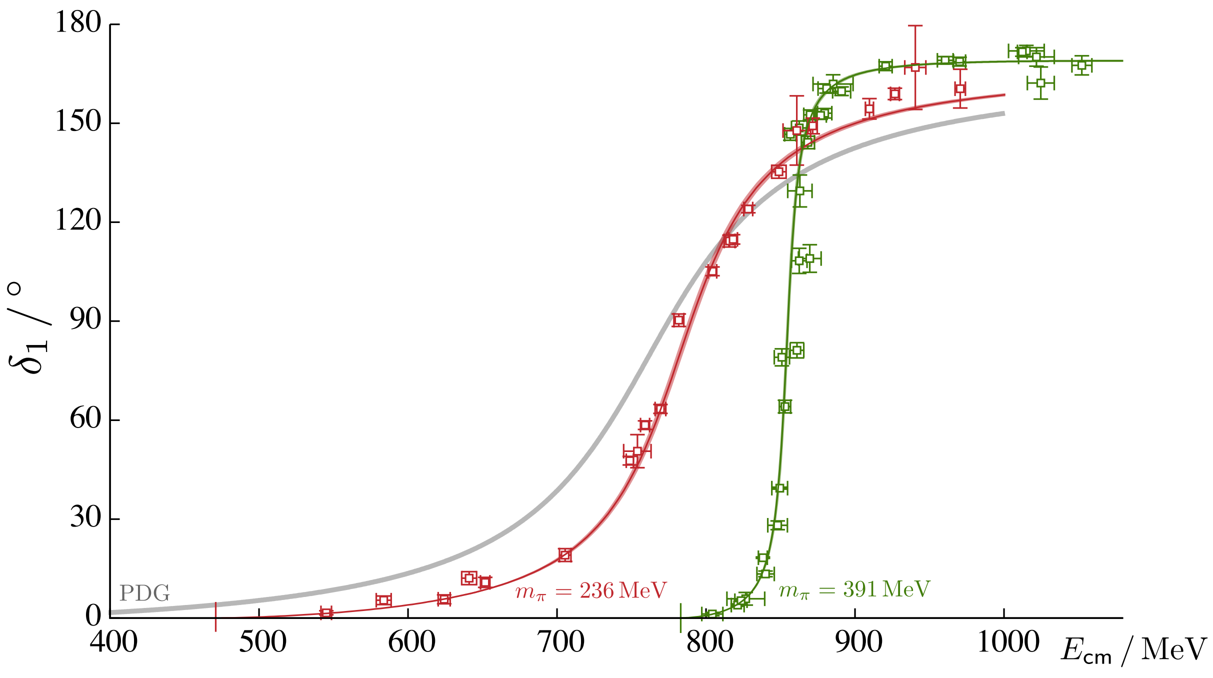


evolution with changing quark mass

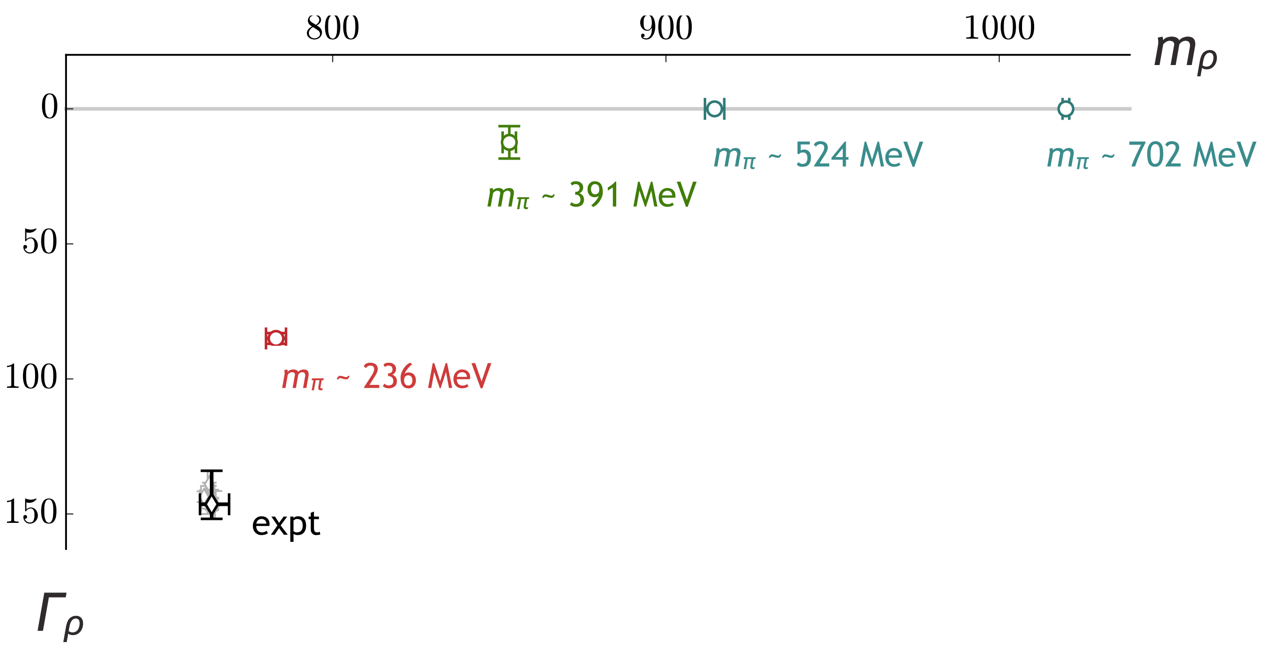

# singularity structure from lattice calculations — elastic

$\pi\pi$ isospin=0

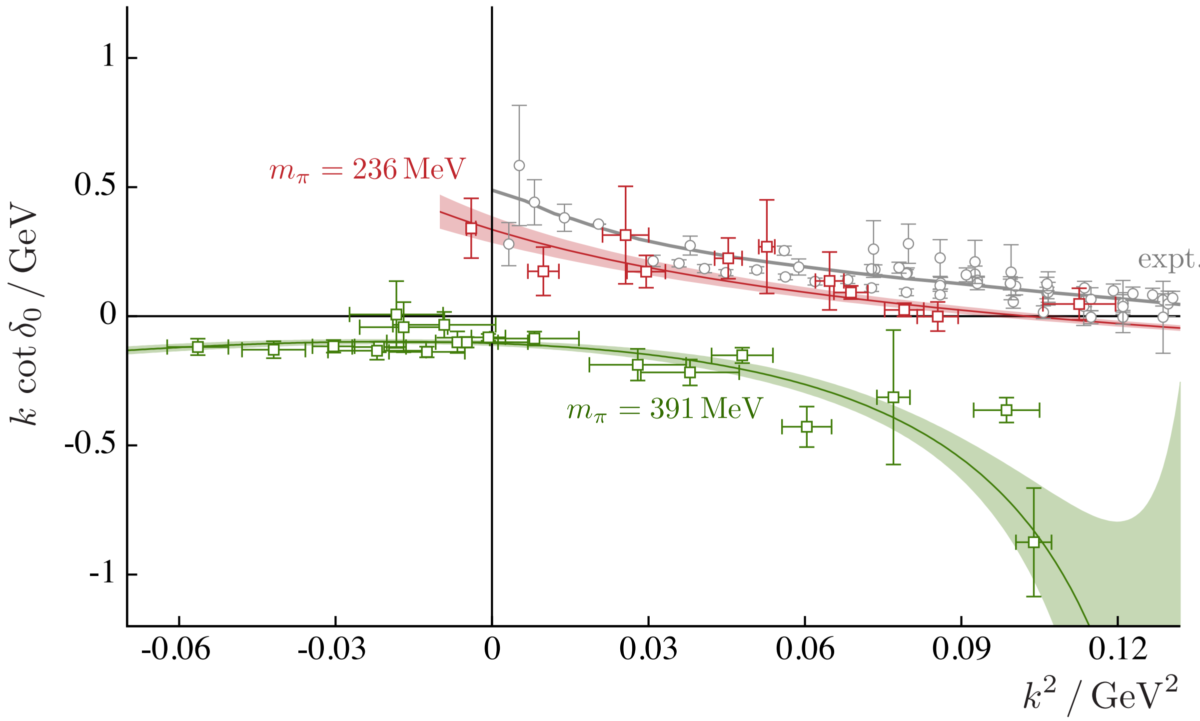


PRL118 022002 (2017)

**$m_\pi$~391 MeV — a bound-state pole**

**$m_\pi$~236 MeV — a resonance pole**

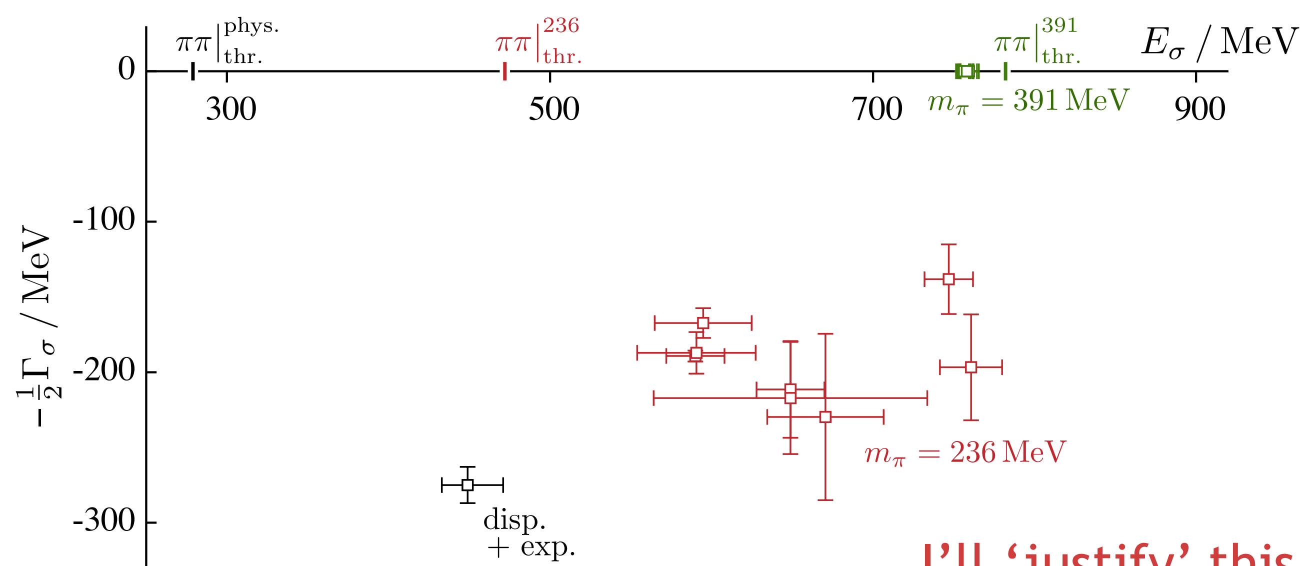


I'll 'justify' this scatter later

# coupled-channels



for each new channel, each sheet splits in two ⇒ $2^N$ sheets for $N$ channels

e.g. two channels

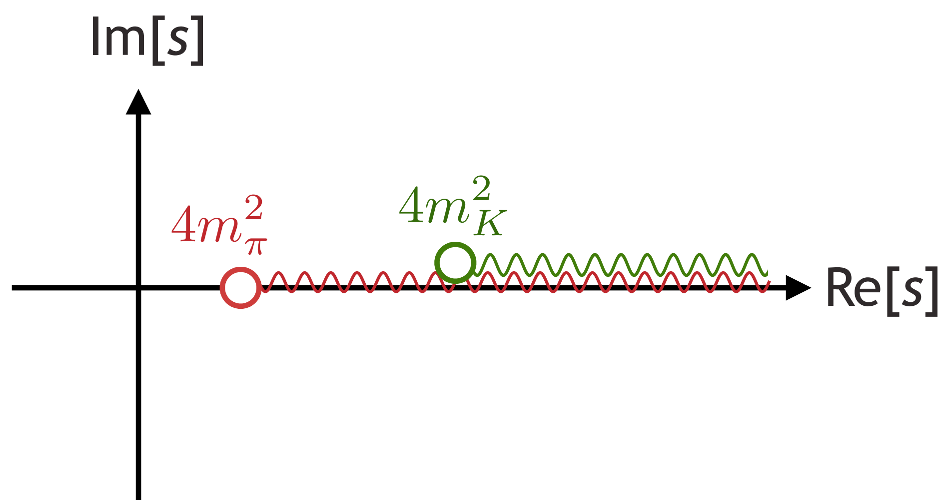

# coupled-channels

for each new channel, each sheet splits in two ⇒ $2^N$ sheets for $N$ channels

e.g. two channels

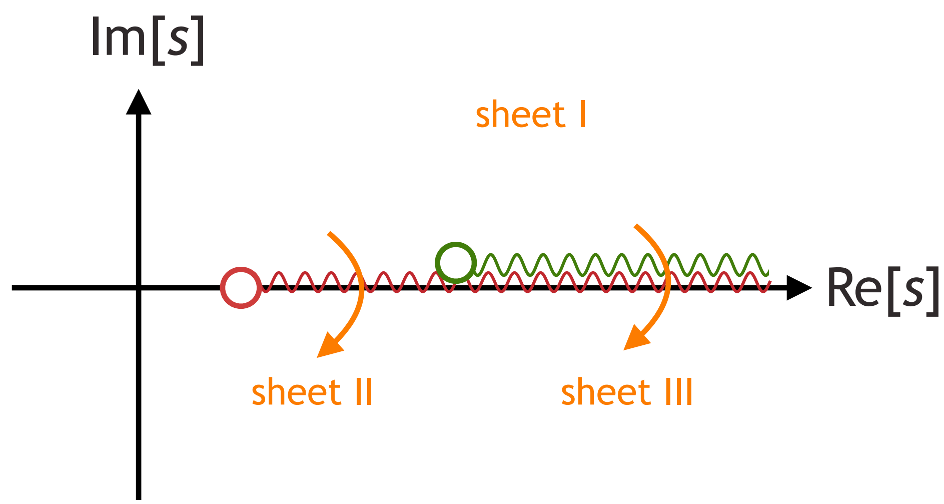


| | Im[ $k_{\pi\pi}$ ] | Im[ $k_{KK}$ ] |
|---|---|---|
| sheet I | + | + |
| sheet II | − | + |
| sheet III | − | − |
| sheet IV | + | − |

# coupled-channels

for each new channel, each sheet splits in two ⇒ $2^N$ sheets for $N$ channels

e.g. two channels

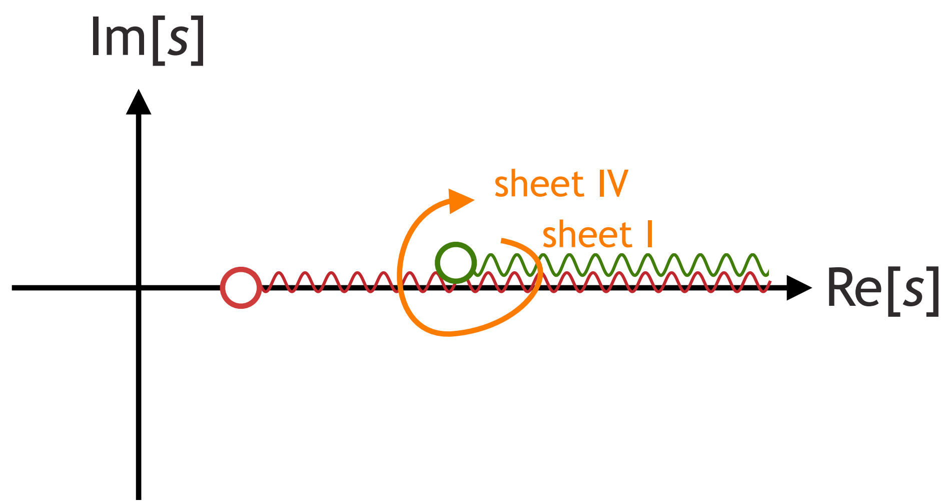


| | Im[ $k_{\pi\pi}$ ] | Im[ $k_{KK}$ ] |
|---|---|---|
| sheet I | + | + |
| sheet II | − | + |
| sheet III | − | − |
| sheet IV | + | − |

# coupled-channels



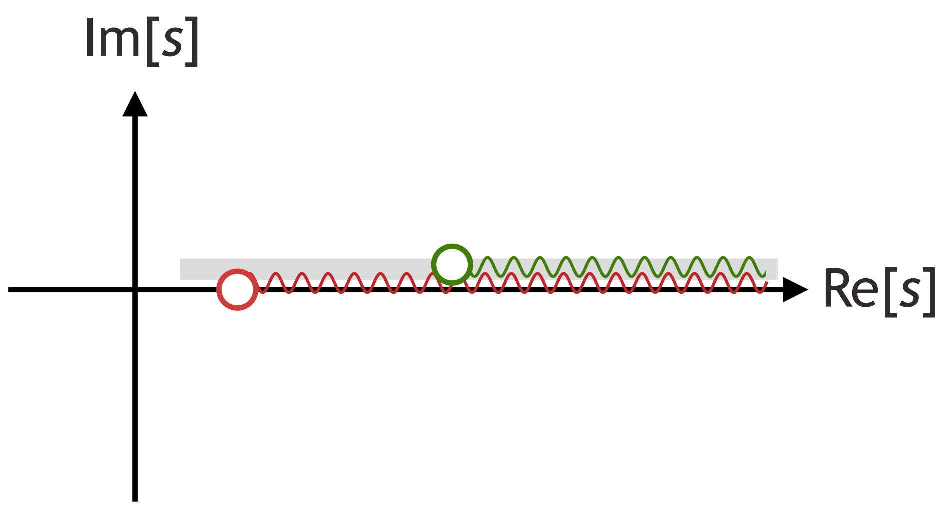


| | Im[ $k_{\pi\pi}$ ] | Im[ $k_{KK}$ ] |
|---|---|---|
| sheet I | + | + |
| sheet II | − | + |
| sheet III | − | − |
| sheet IV | + | − |

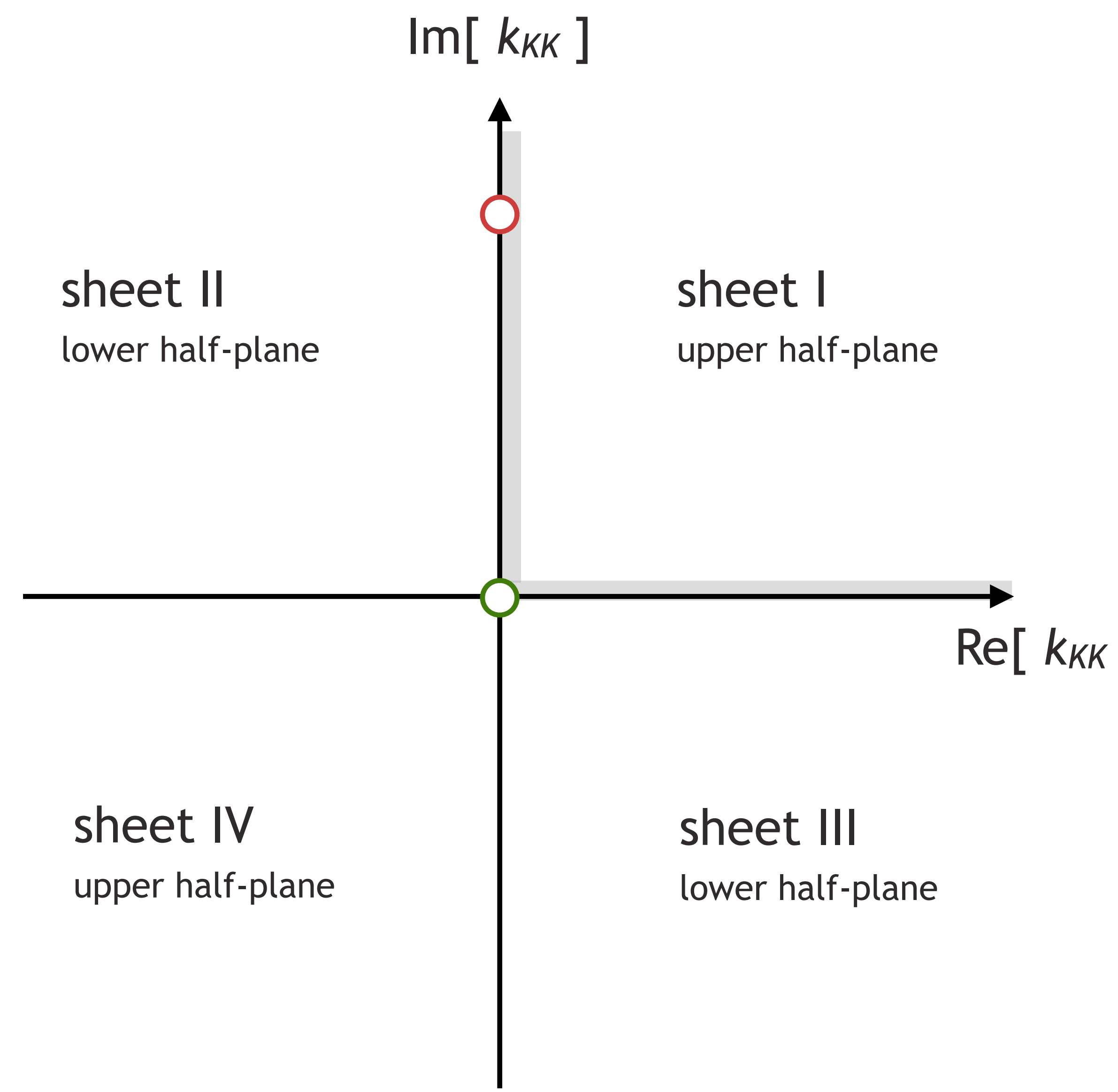

# two-channel Flatté amplitude

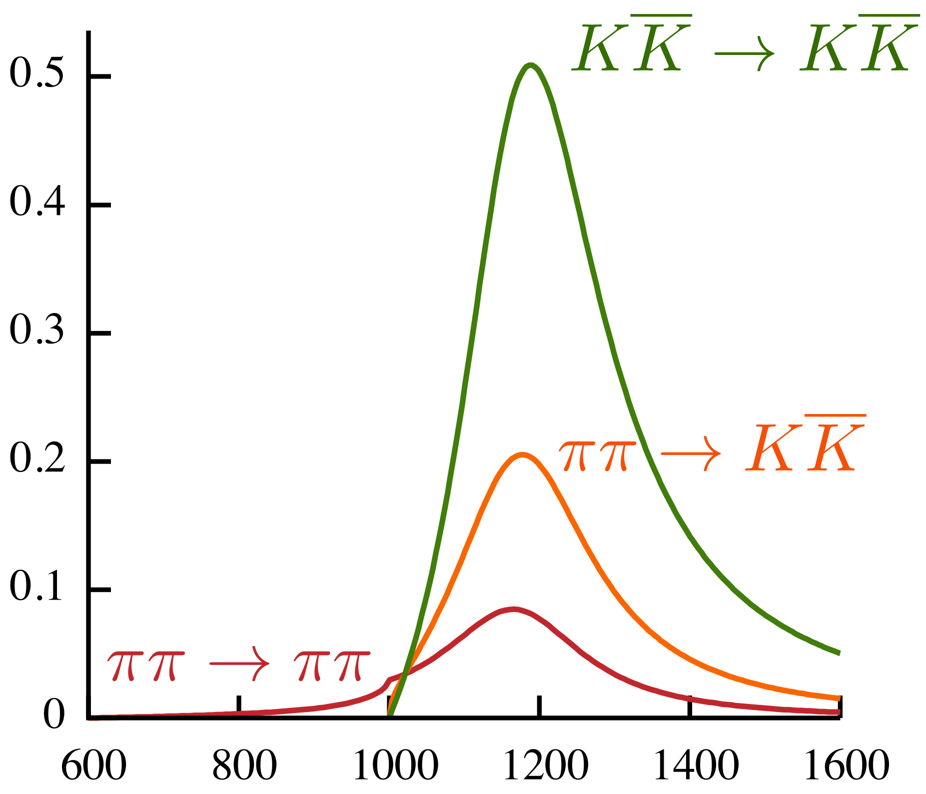


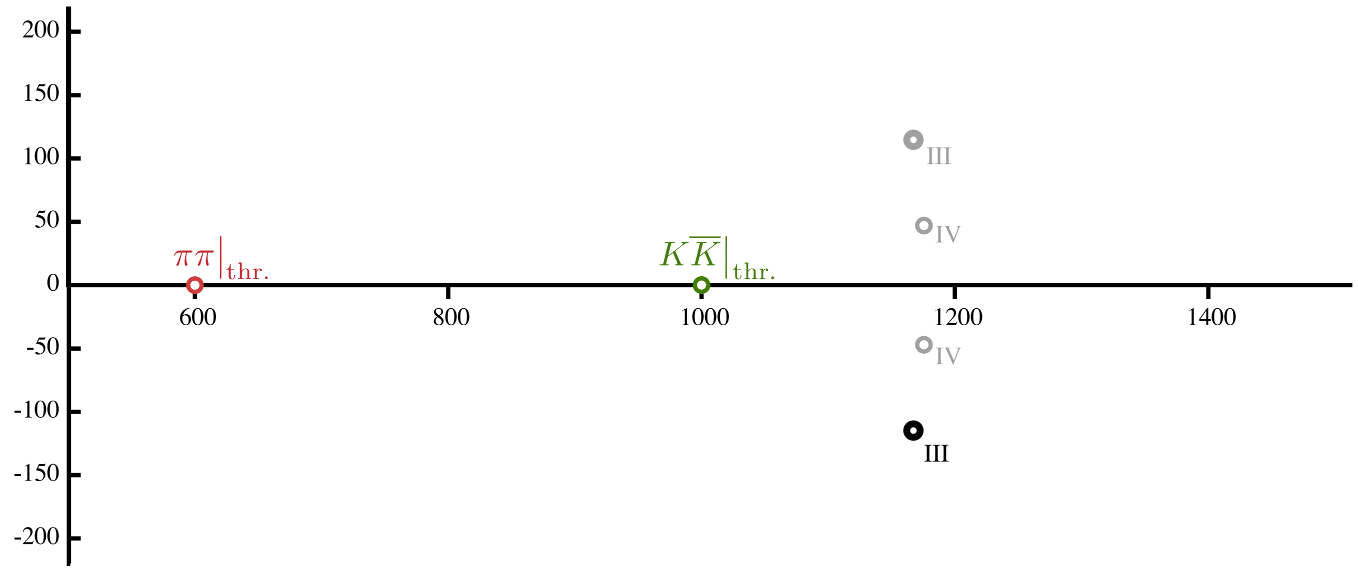


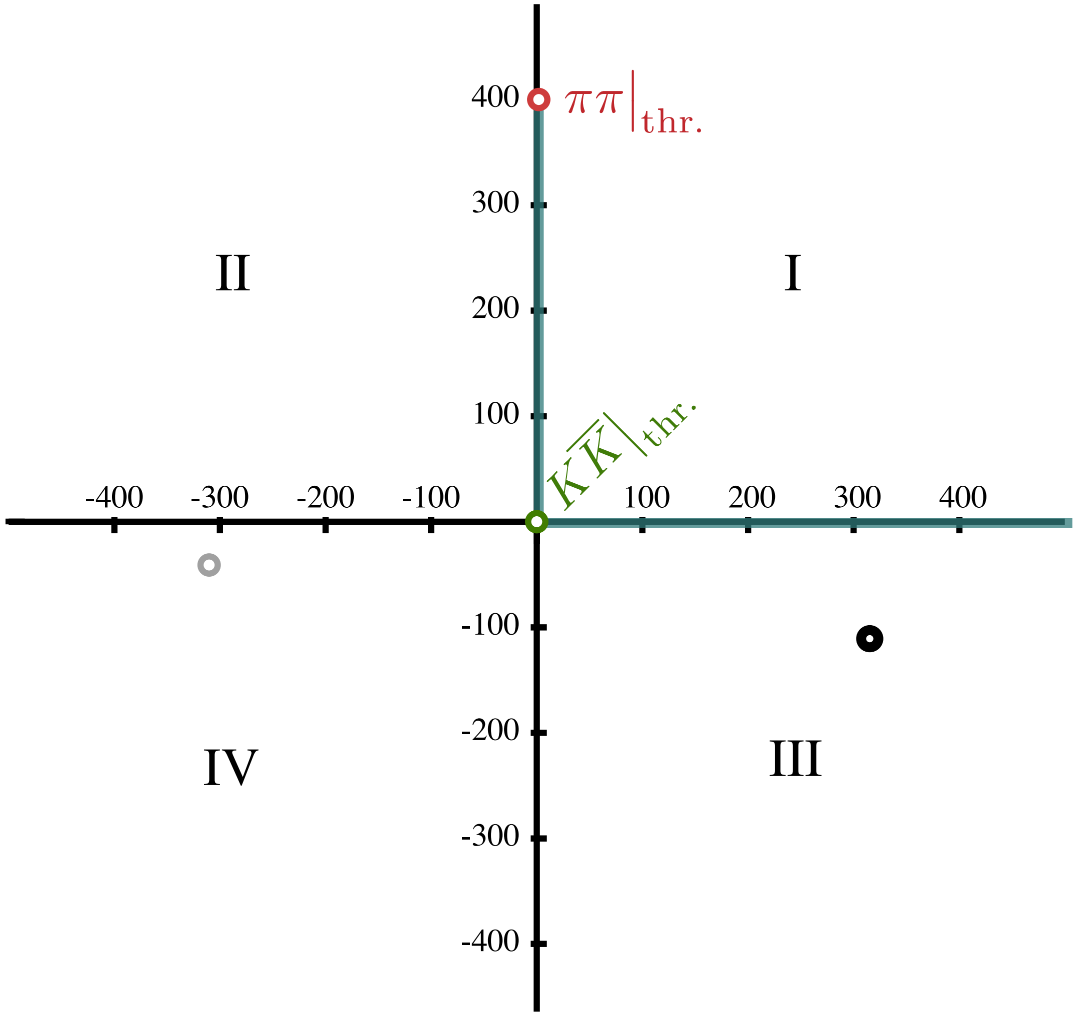

# a less obviously resonant amplitude

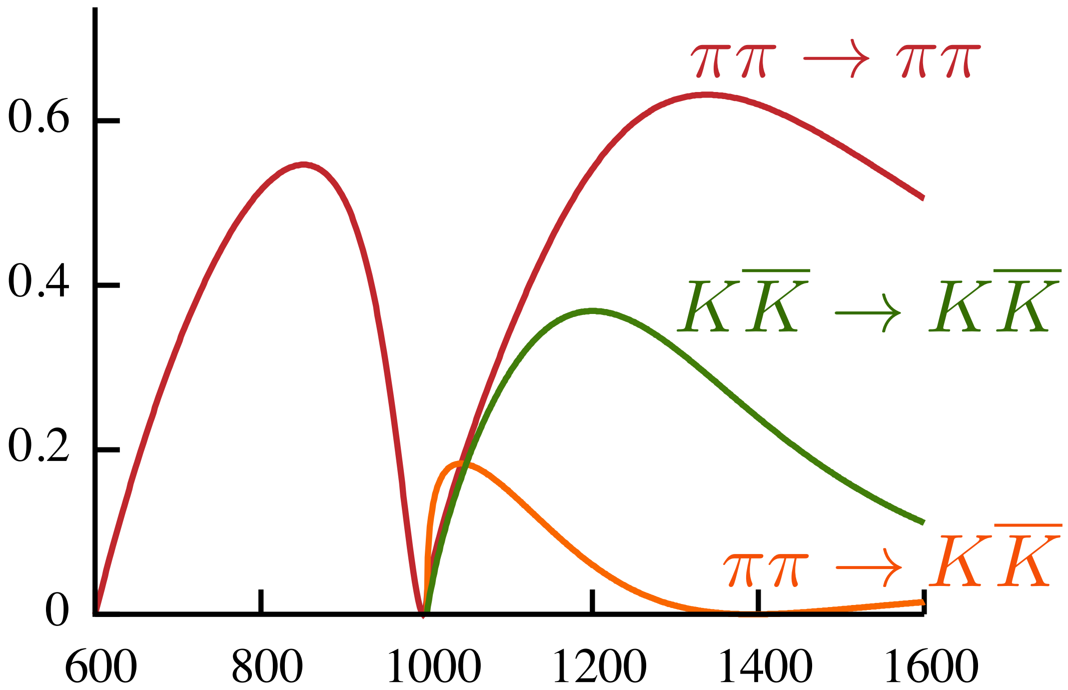


$$\mathbf{K}^{-1}(s) = \begin{pmatrix} a & b + c\,s \\ b + c\,s & d + e\,s \end{pmatrix}$$

with Chew-Mandelstam phase-space

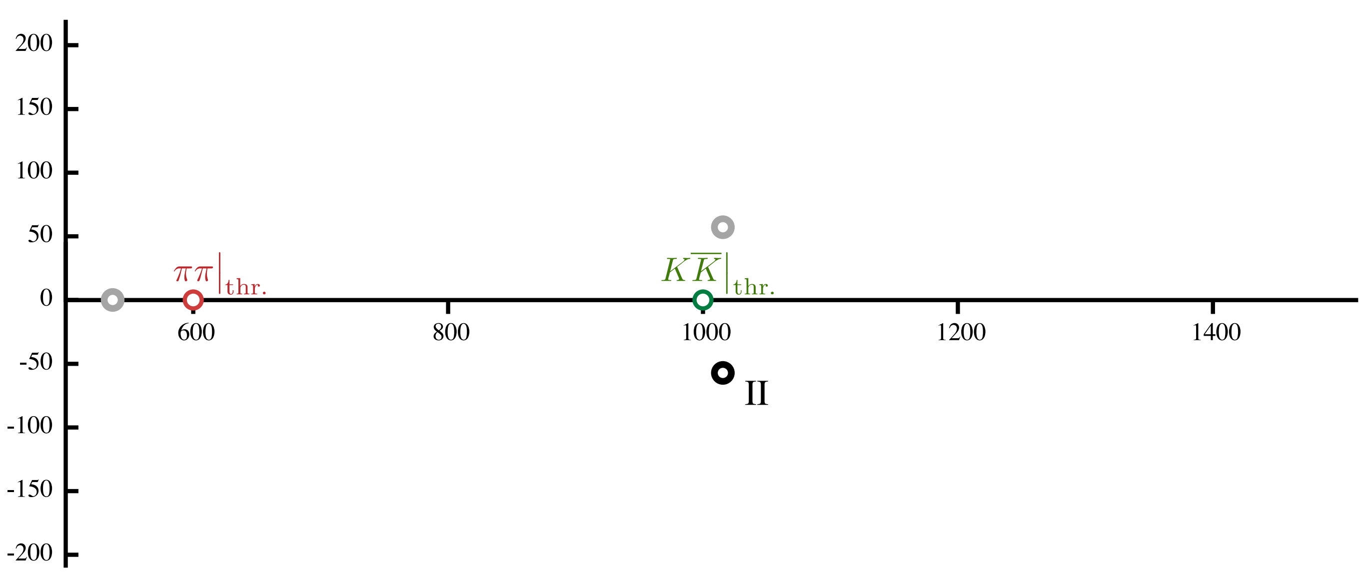


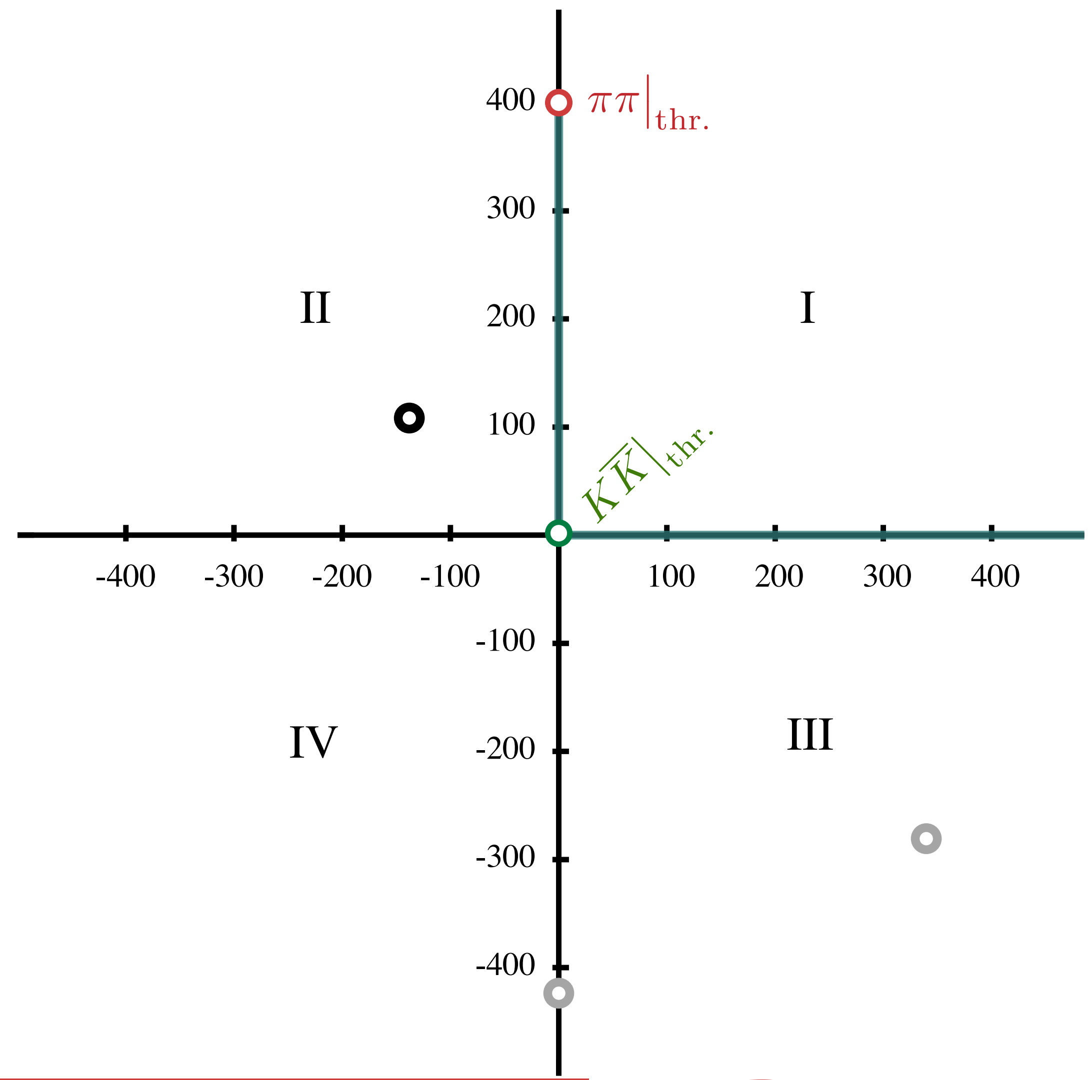

# information from the pole

near the complex pole, $s_0$

$$t_{ij}(s \sim s_0) \sim \frac{c_i\, c_j}{s_0 - s}$$

pole **position** can be interpreted as **mass** and **width**

$$s_0 = \left(m_R \pm i\tfrac{1}{2}\Gamma_R\right)^2$$

pole **residue** factorizes into a product of resonance **couplings** to the various decay channels

$$c_{\pi\pi},\ c_{K\bar{K}},\ \ldots$$

as we've seen a single resonance can be responsible for poles on more than one sheet

— often only one is close enough to physical scattering to have a large effect

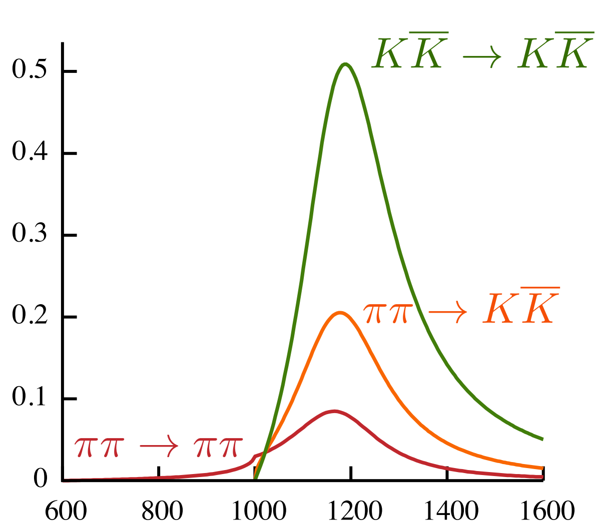


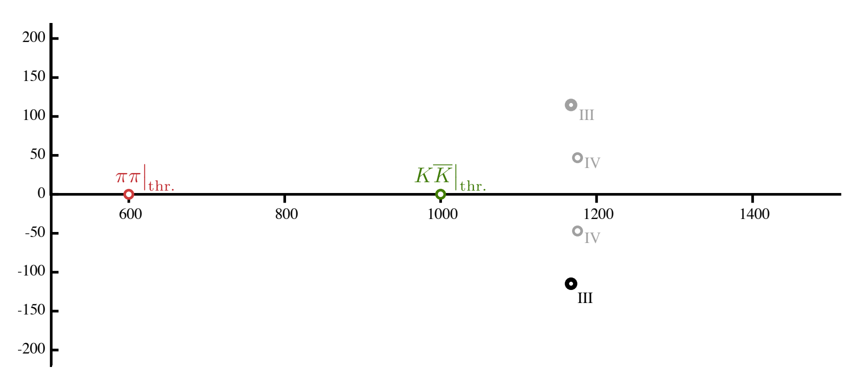


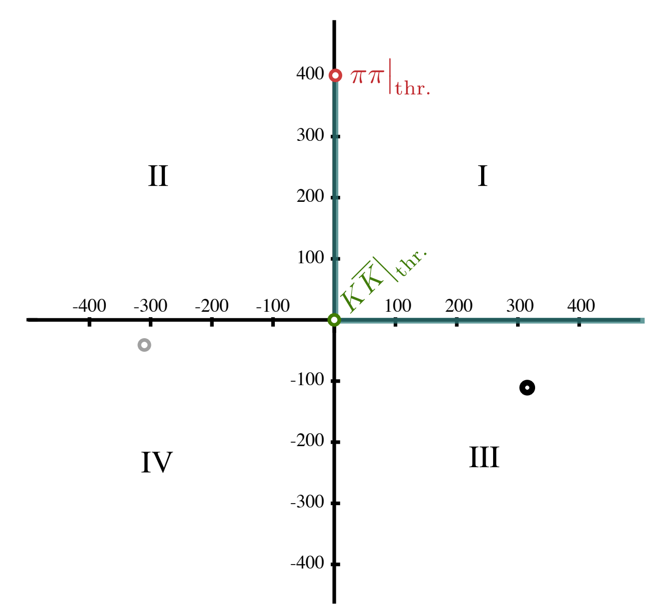

# $\pi\pi$, $K\bar{K}$, $\eta\eta$ scattering with $m_\pi$~391 MeV

PRD 97 054513 (2018)

## S-wave amplitudes

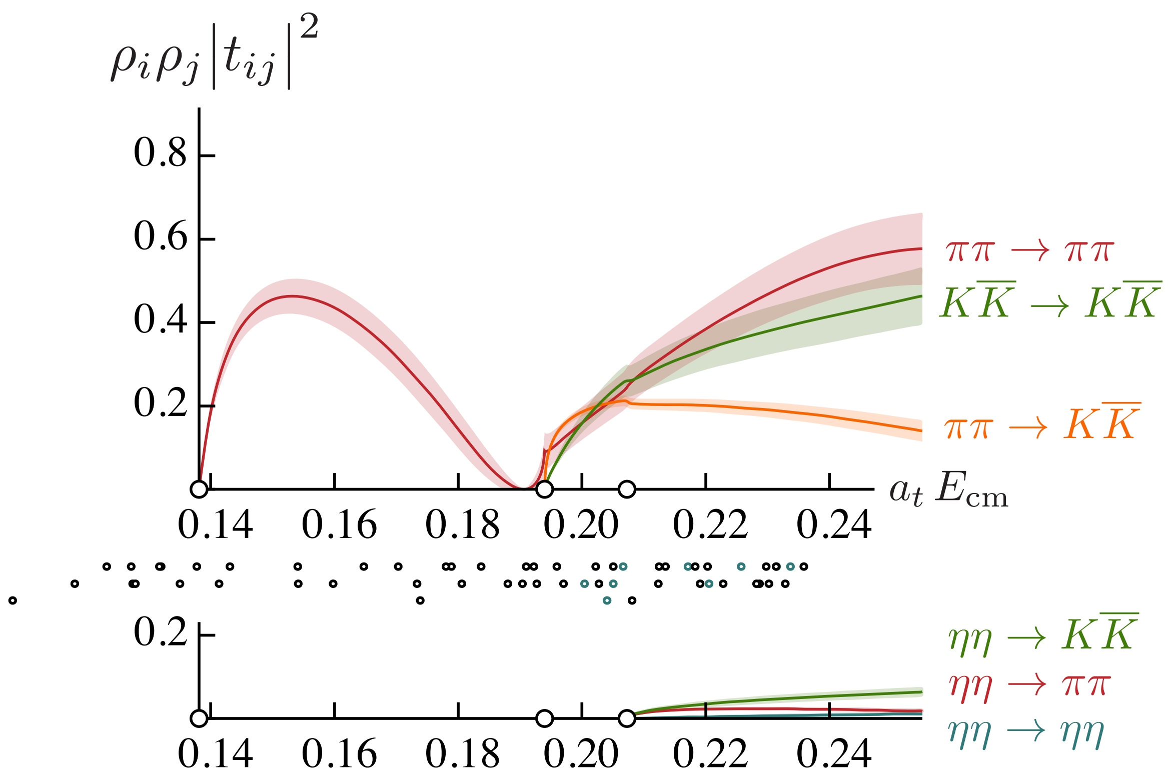


$$\mathbf{K}^{-1}(s) = \begin{pmatrix} a + b\,s & c + d\,s & e \\ c + d\,s & f & g \\ e & g & h \end{pmatrix}$$

with Chew-Mandelstam phase-space

## pole singularities

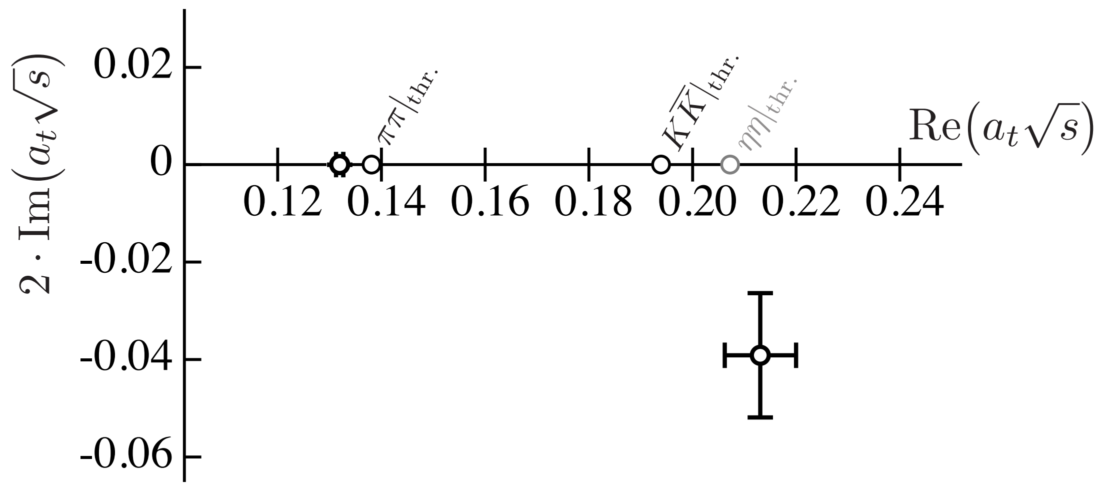


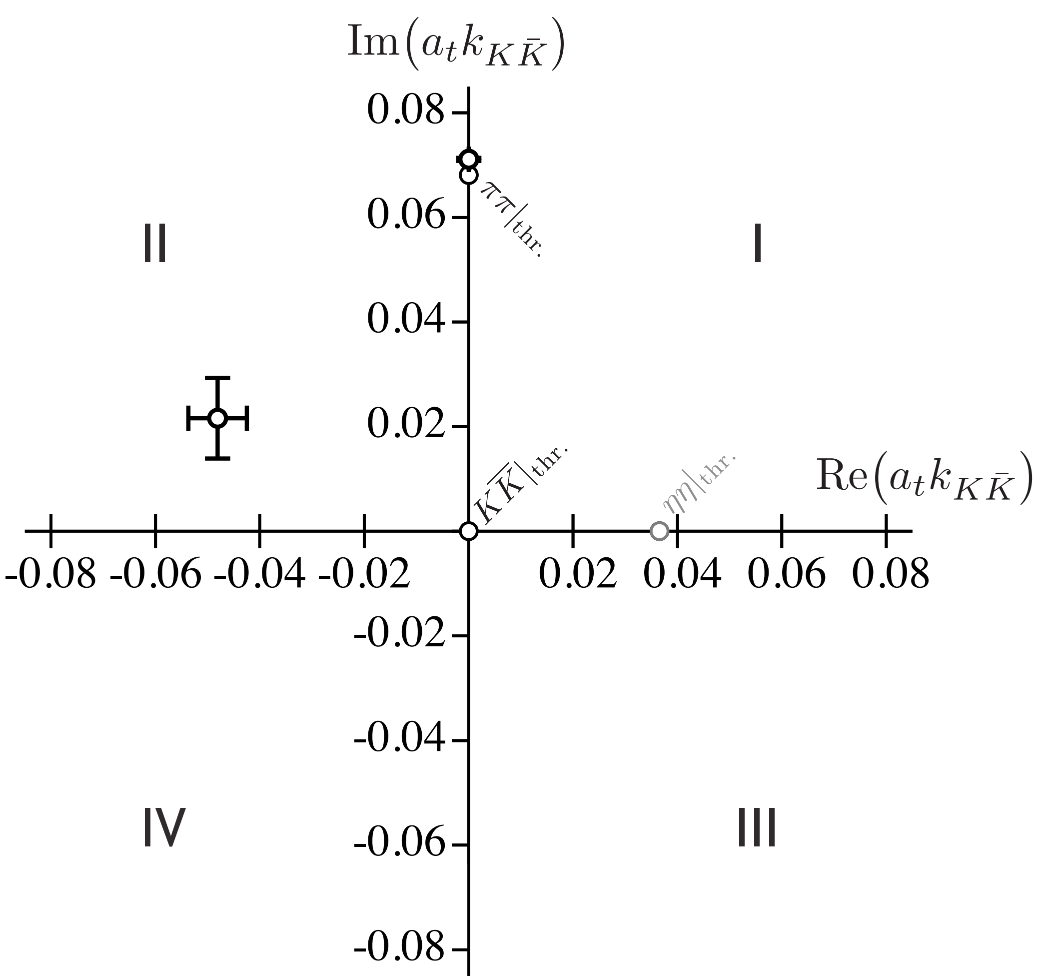

# $\pi\pi$, $K\bar{K}$, $\eta\eta$ scattering with $m_\pi$~391 MeV

PRD 97 054513 (2018)



## S-wave amplitudes

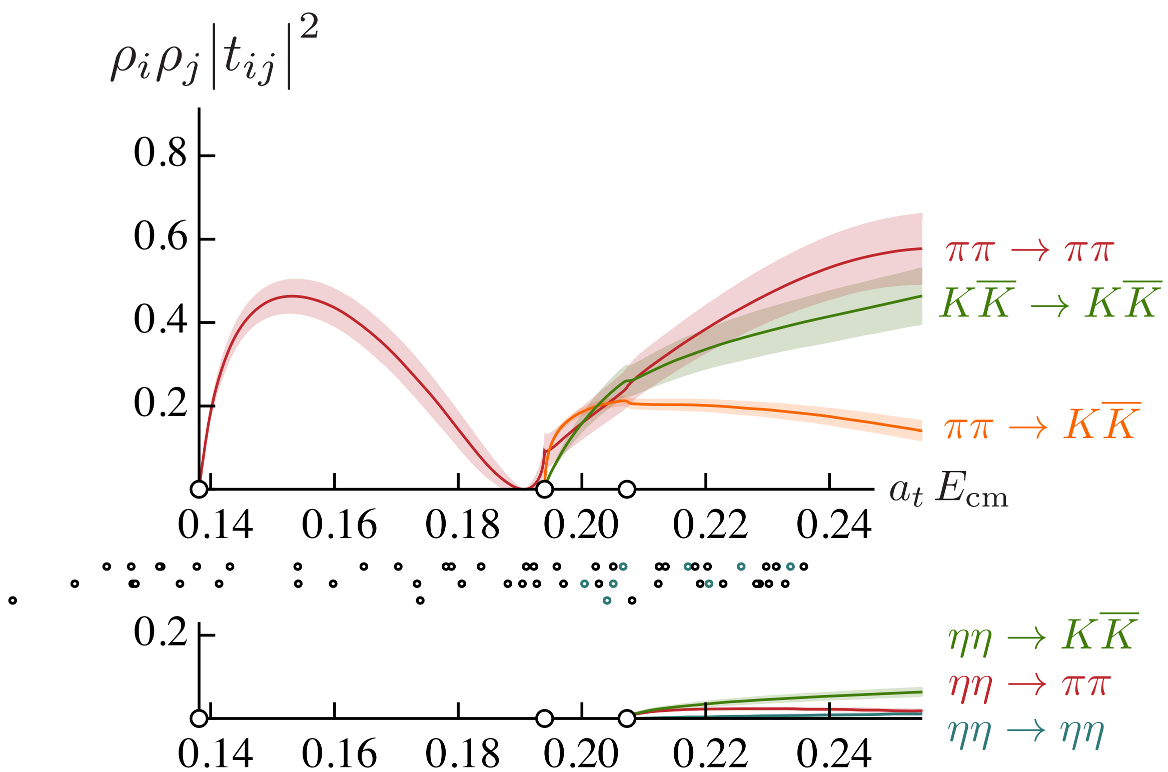


$$\mathbf{K}^{-1}(s) = \begin{pmatrix} a + b\,s & c + d\,s & e \\ c + d\,s & f & g \\ e & g & h \end{pmatrix}$$

with Chew-Mandelstam phase-space

## pole singularities

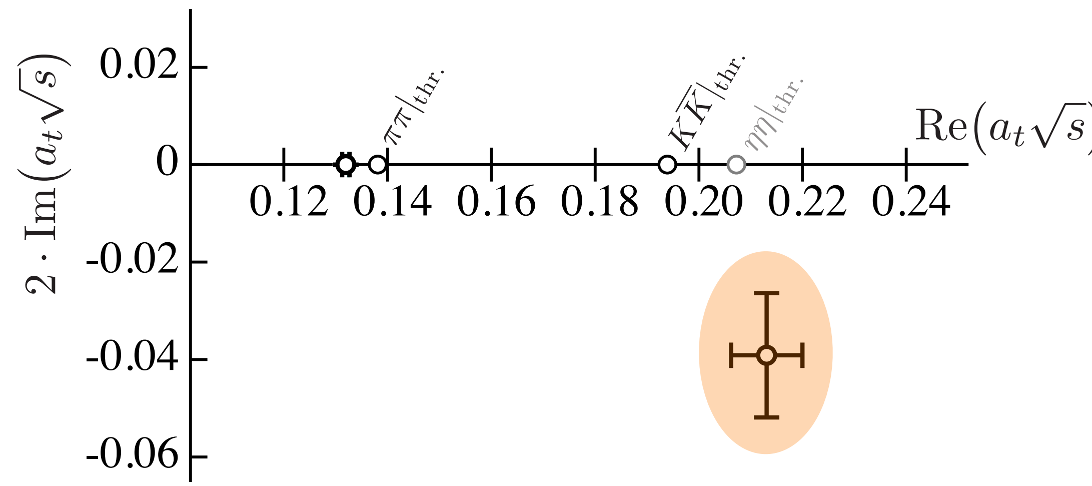


## sheet II pole couplings

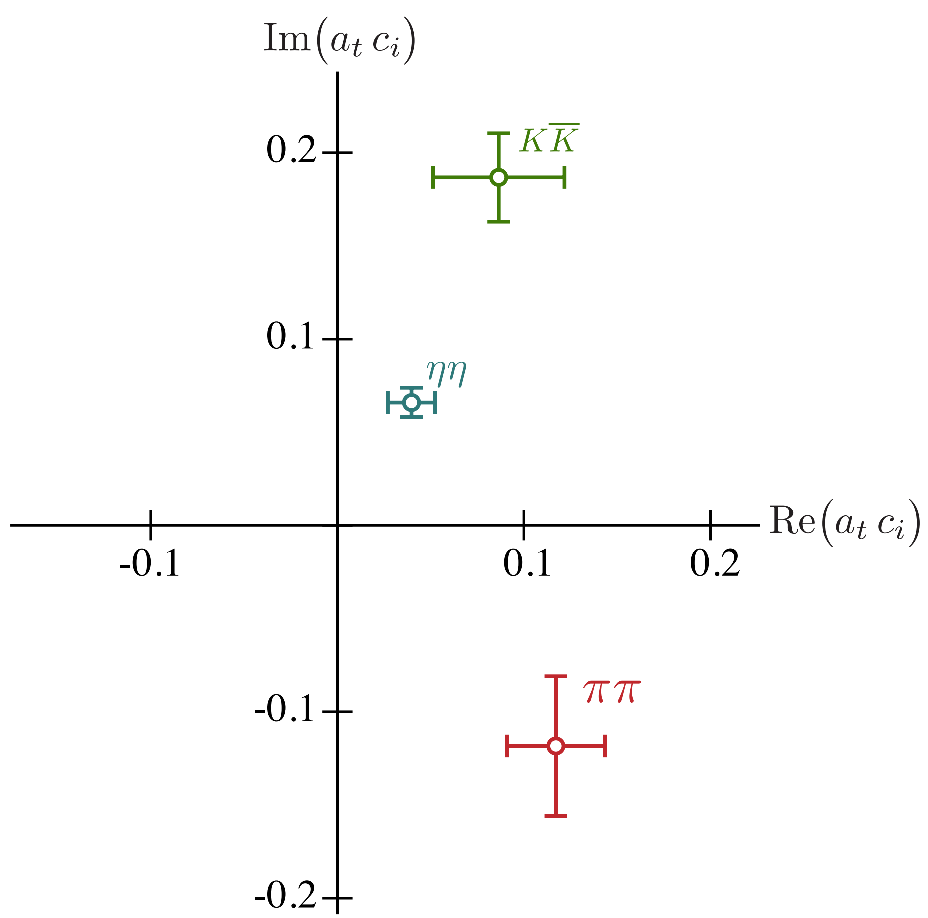

# $\pi\pi$, $K\bar{K}$, $\eta\eta$ scattering with $m_\pi$~391 MeV

PRD 97 054513 (2018)



## S-wave amplitudes

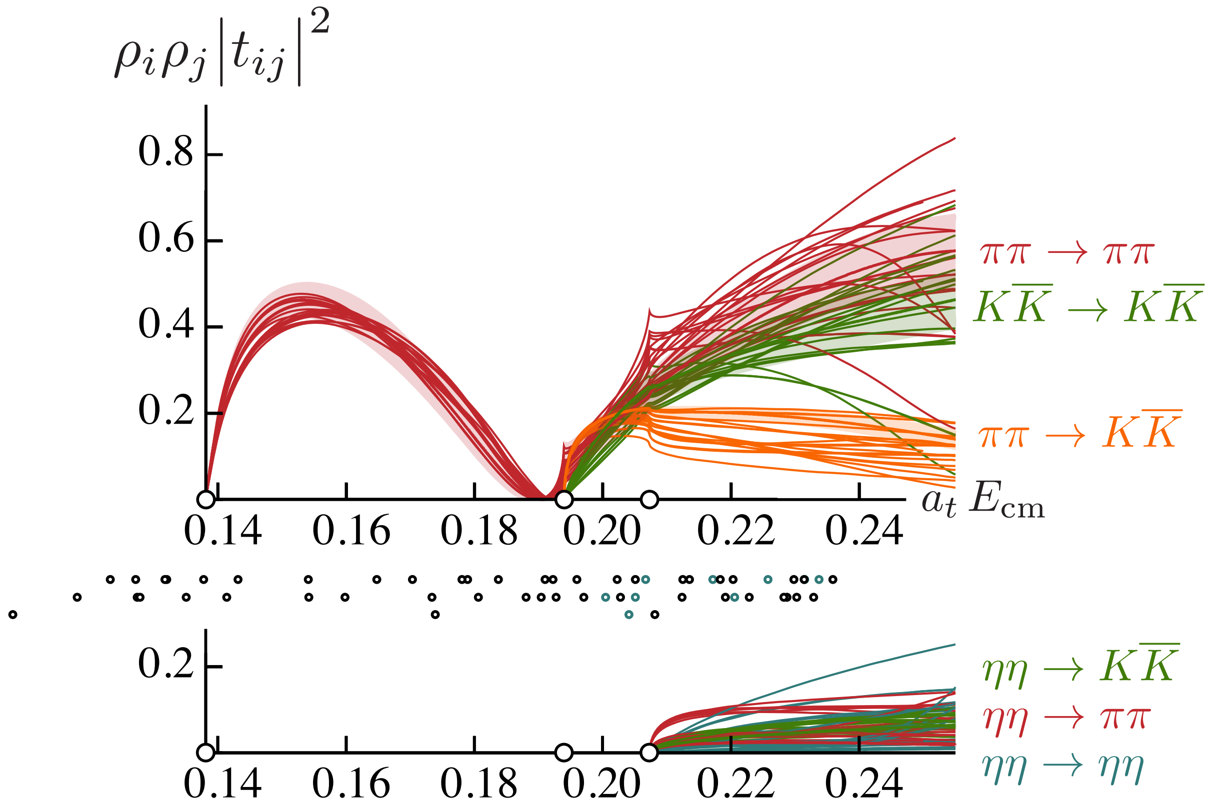


## pole singularities

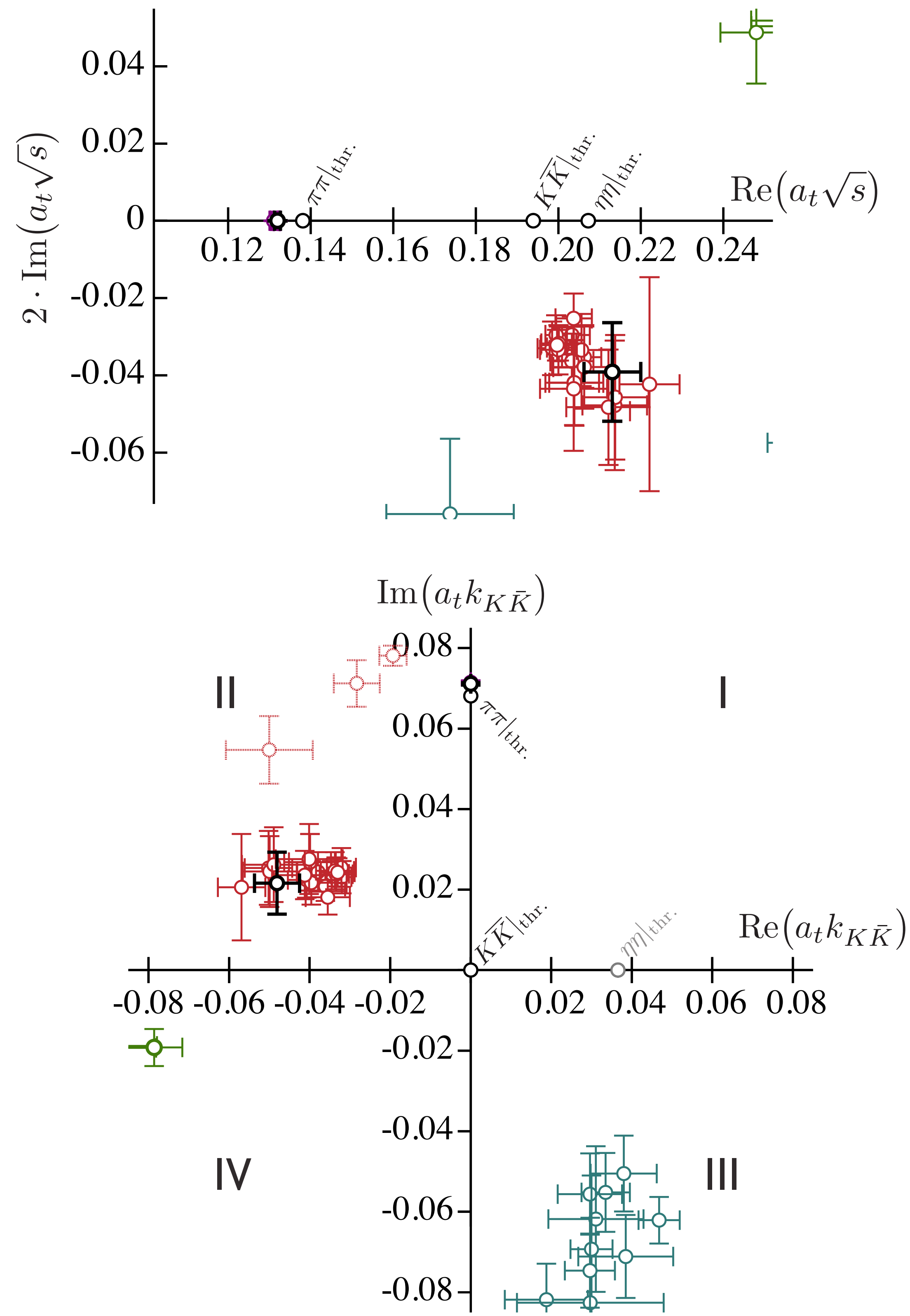

# $\pi\pi$, $K\bar{K}$, $\eta\eta$ scattering with $m_\pi$~391 MeV

summary, including spread over parameterizations in pole uncertainty

S-wave amplitudes & poles

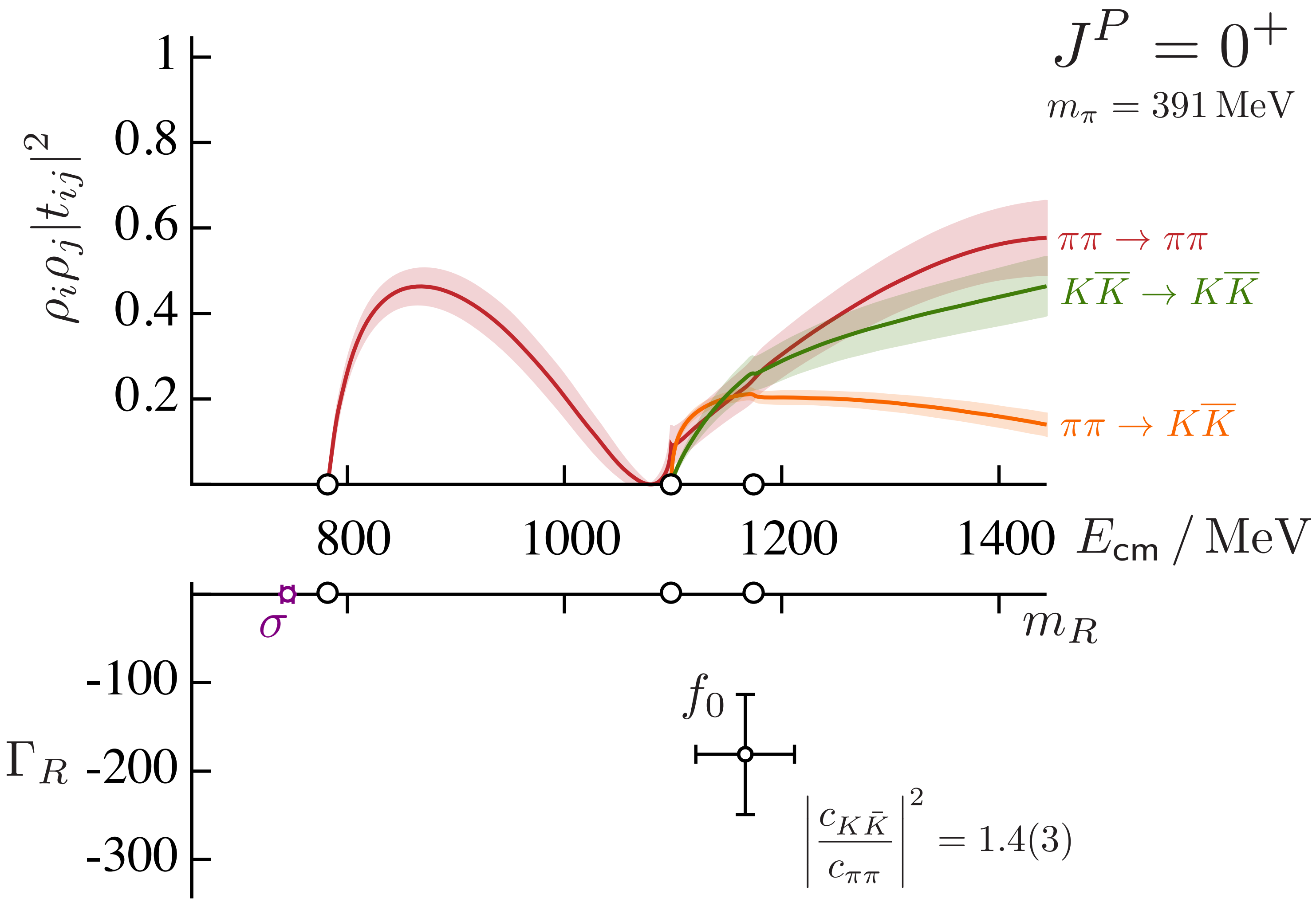


the $f_0$("980")

# singularity structure from lattice calculations — elastic

## $\pi\pi$ isospin=0

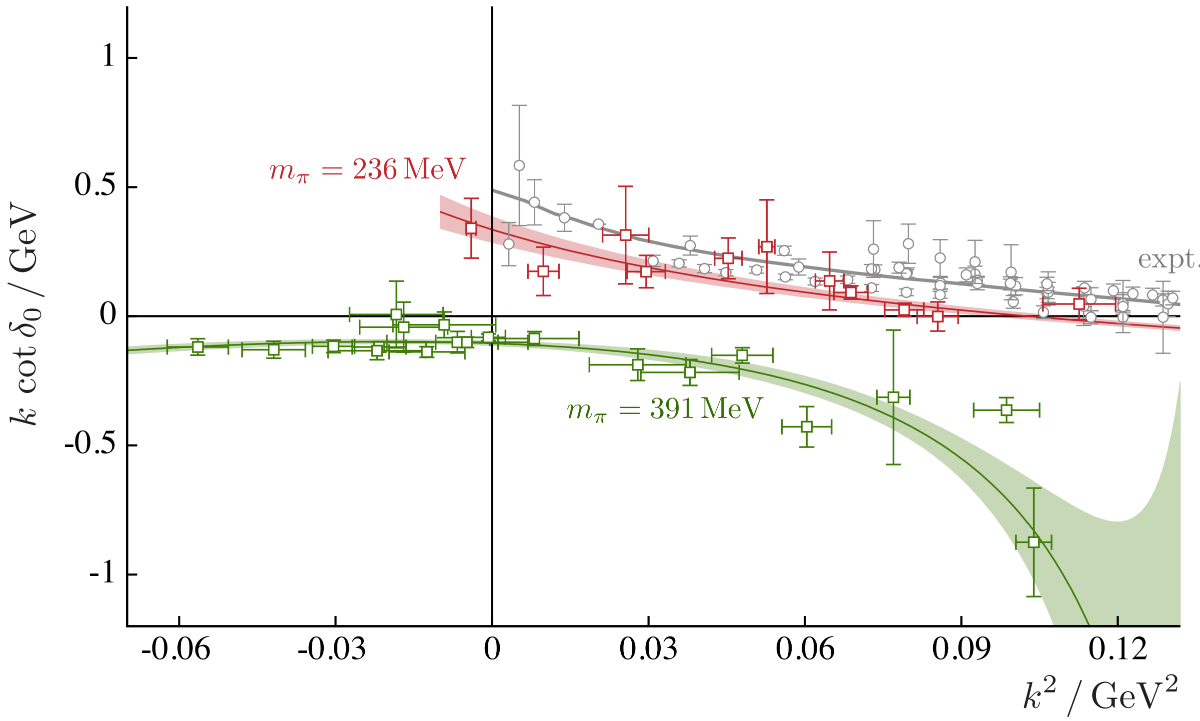


PRL118 022002 (2017)

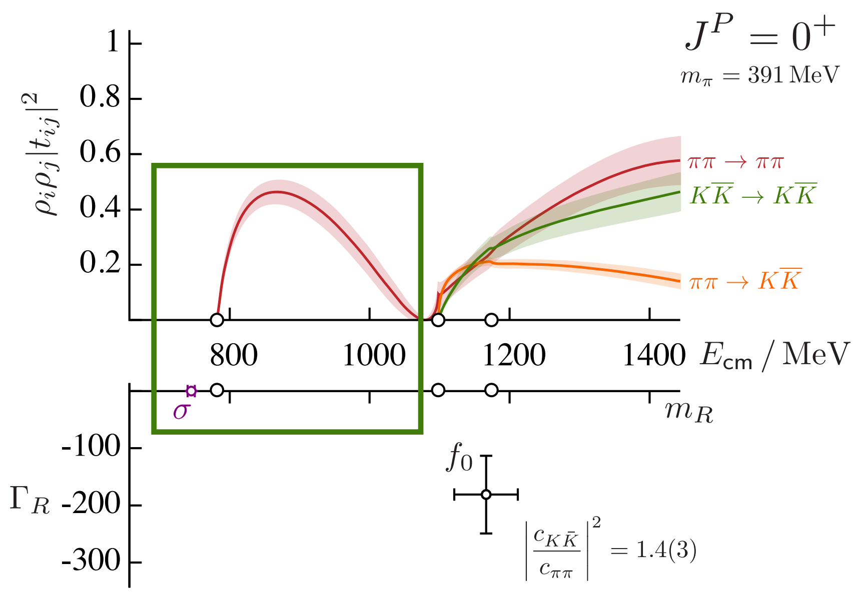


**$m_\pi$~391 MeV — a bound-state pole**

**$m_\pi$~236 MeV — a resonance pole**

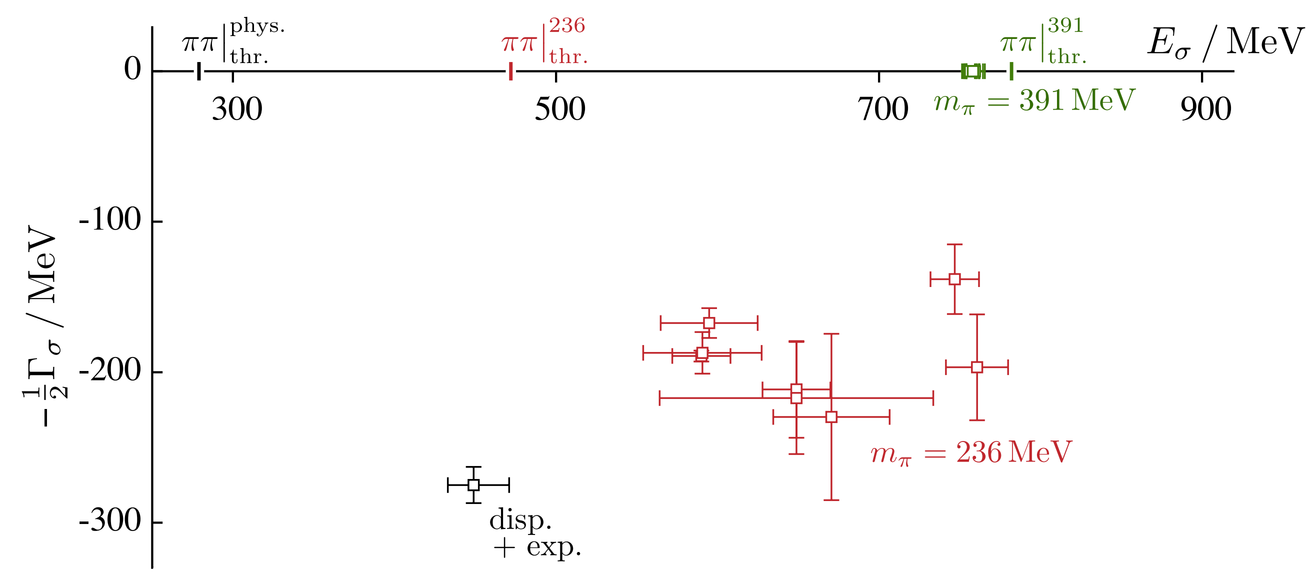

similar calculation in isospin=1, *G*-parity negative channel

S-wave amplitudes

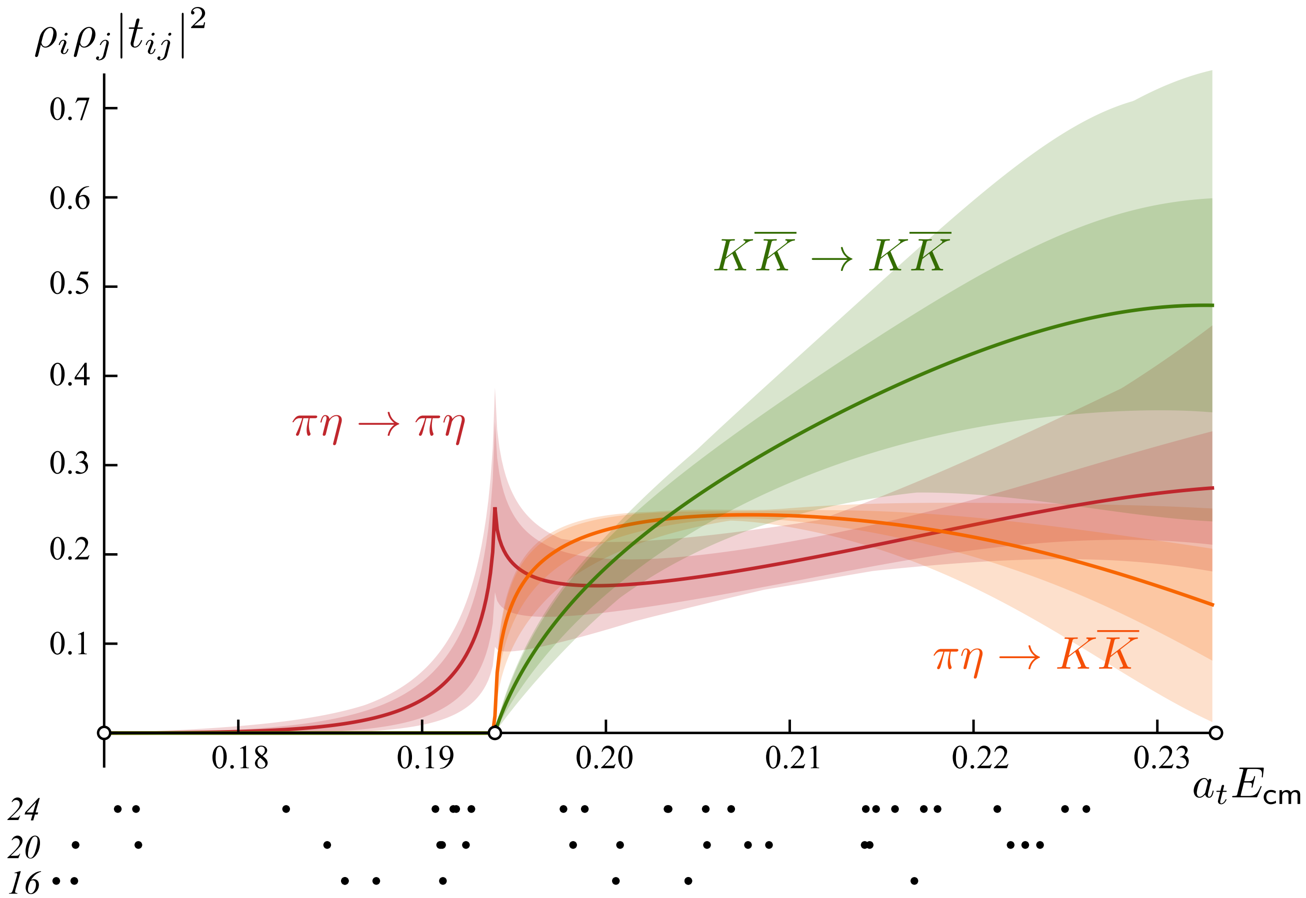


looks very different to isospin=0 case shown before

# $\pi\eta$, $K\overline{K}$ scattering with $m_\pi$~391 MeV

PRD 93 094506 (2016)

## S-wave amplitudes

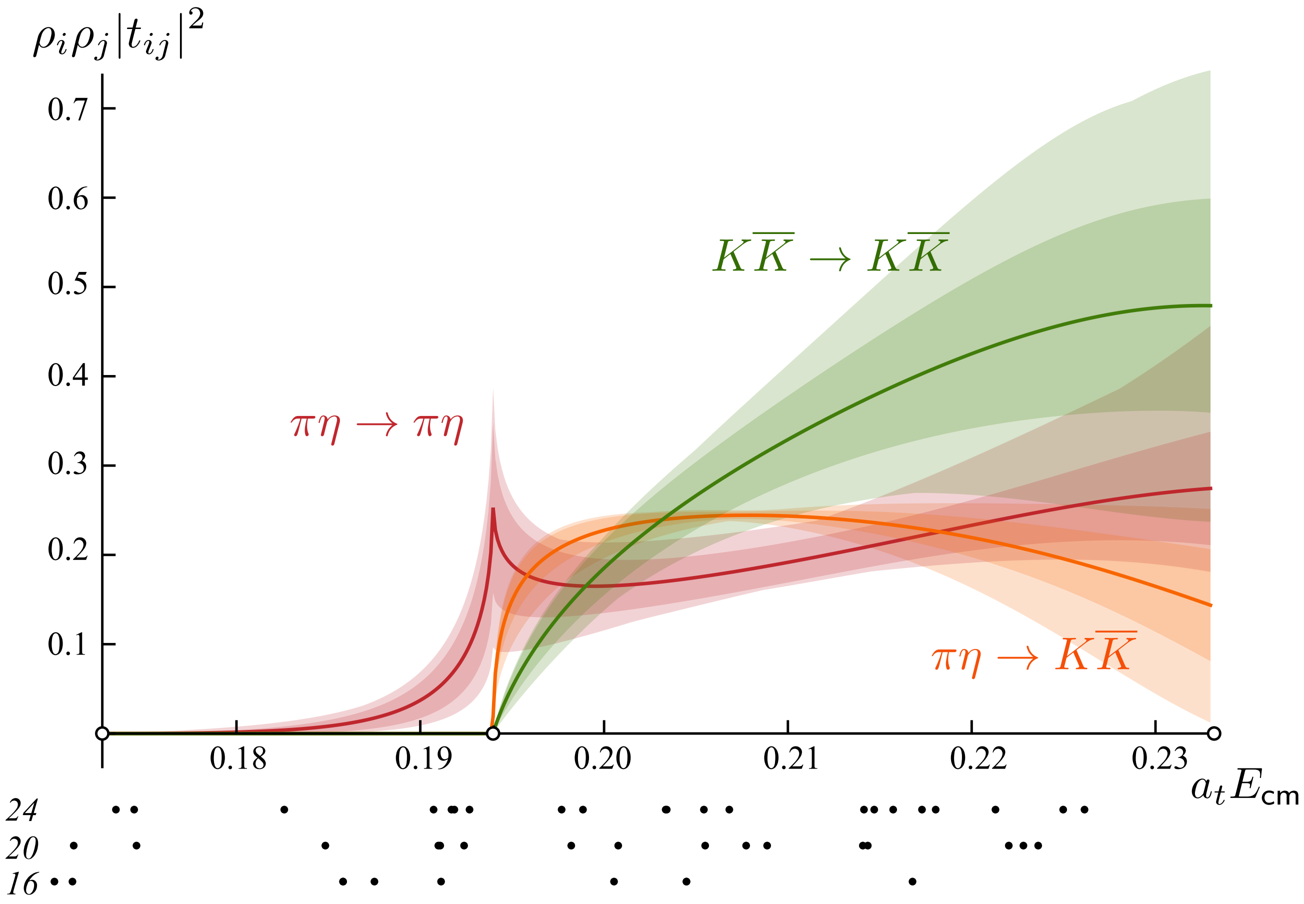


## pole singularities

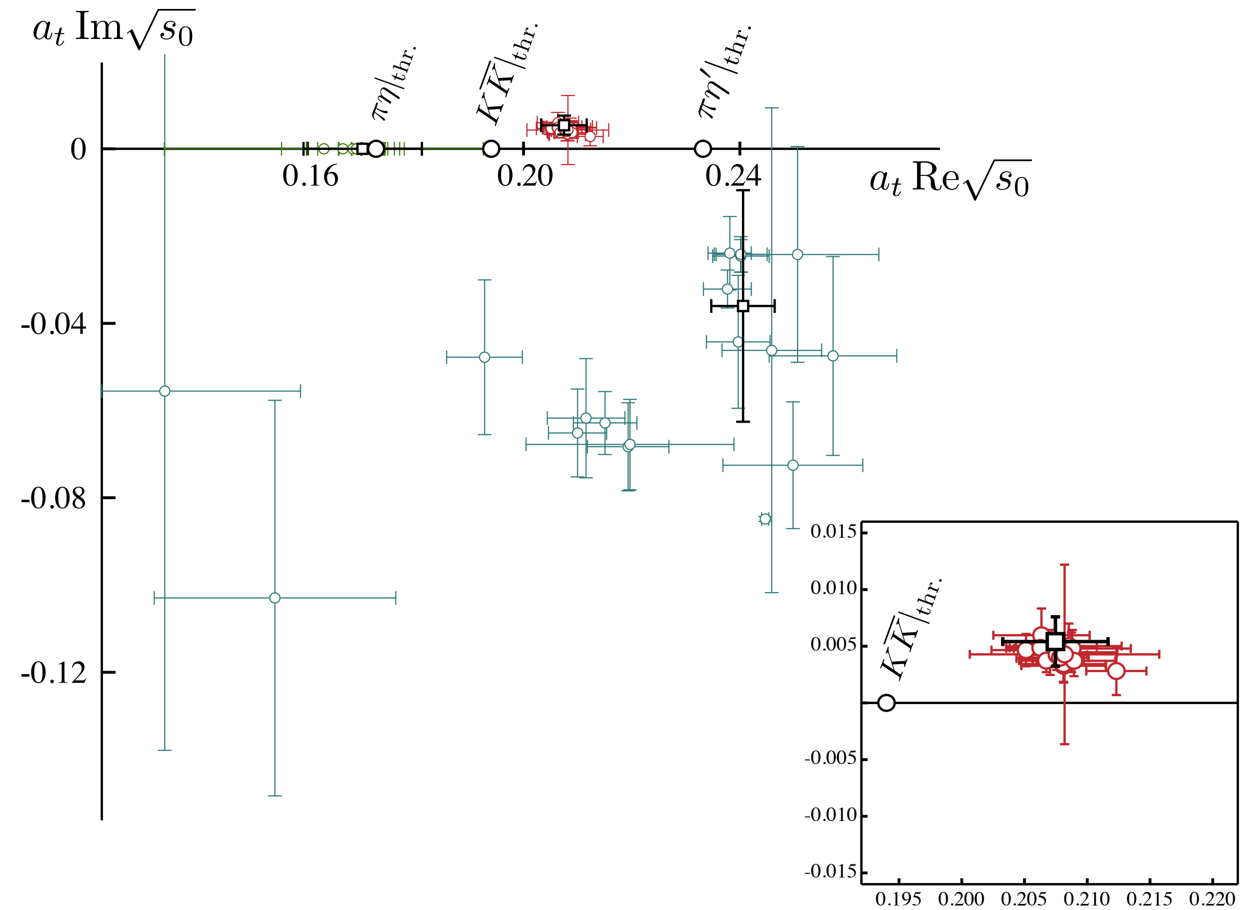

# $\pi\eta$, $K\bar{K}$ scattering with $m_\pi$~391 MeV

## S-wave amplitudes

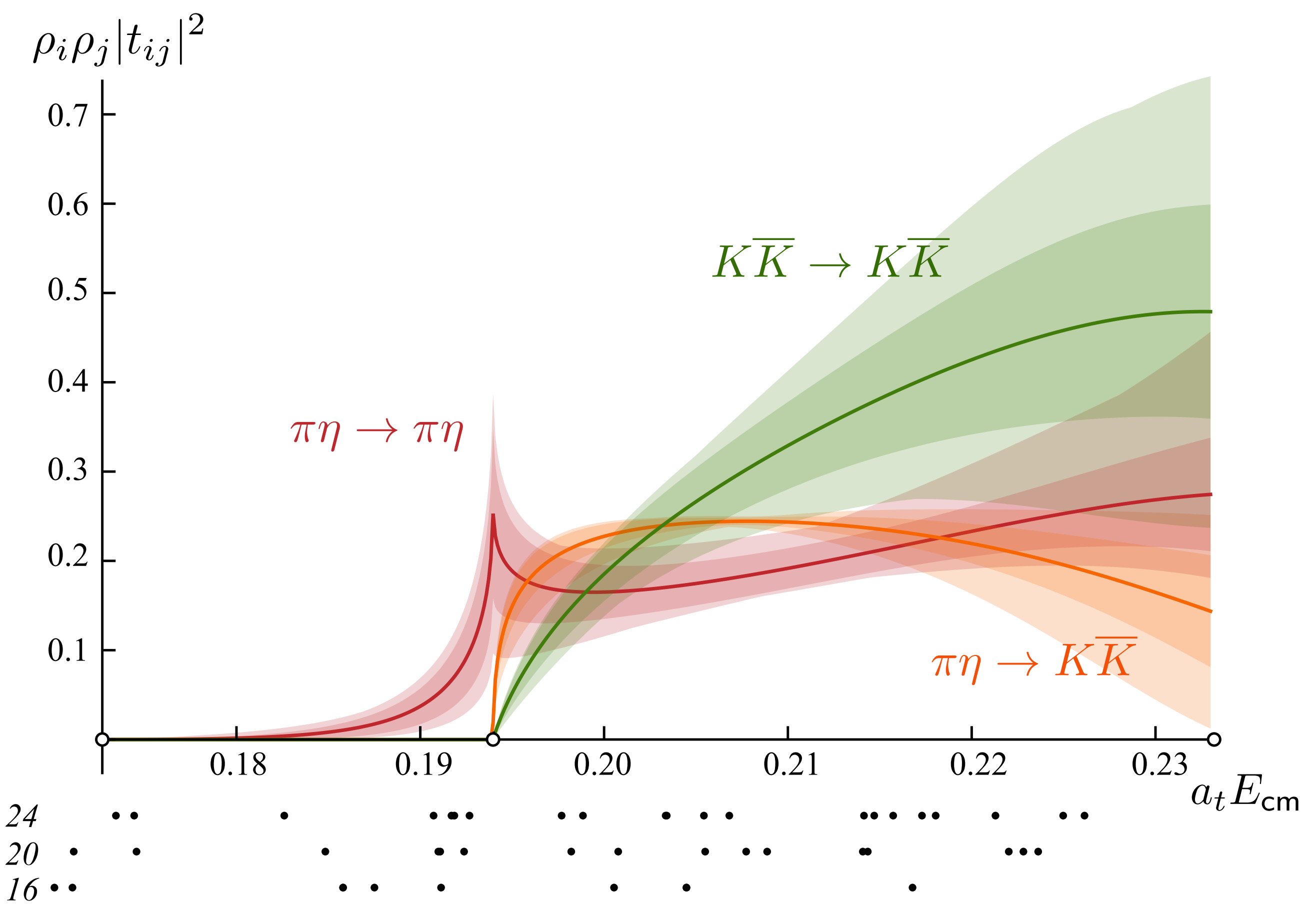


## pole singularities

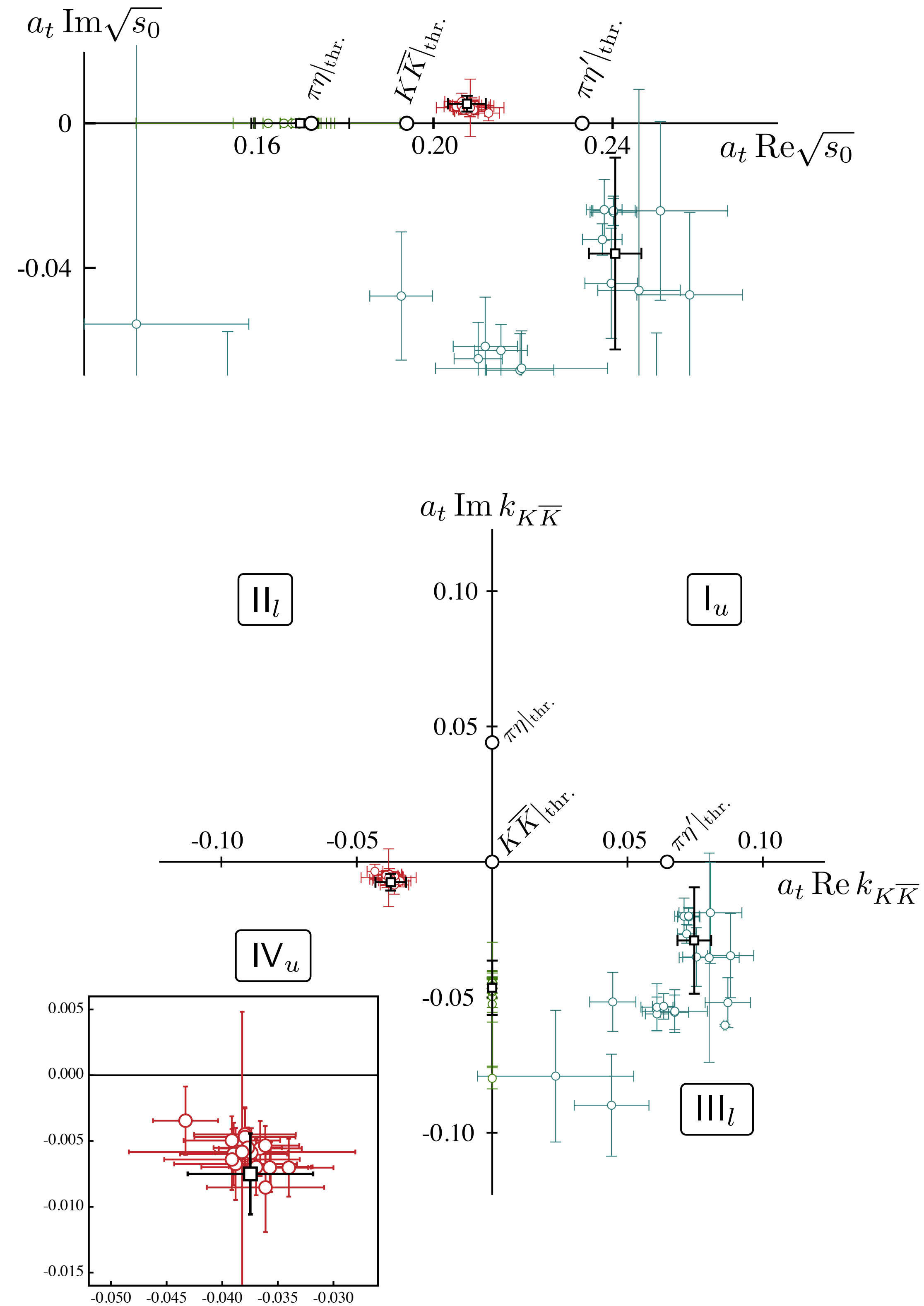

## S-wave amplitudes & poles

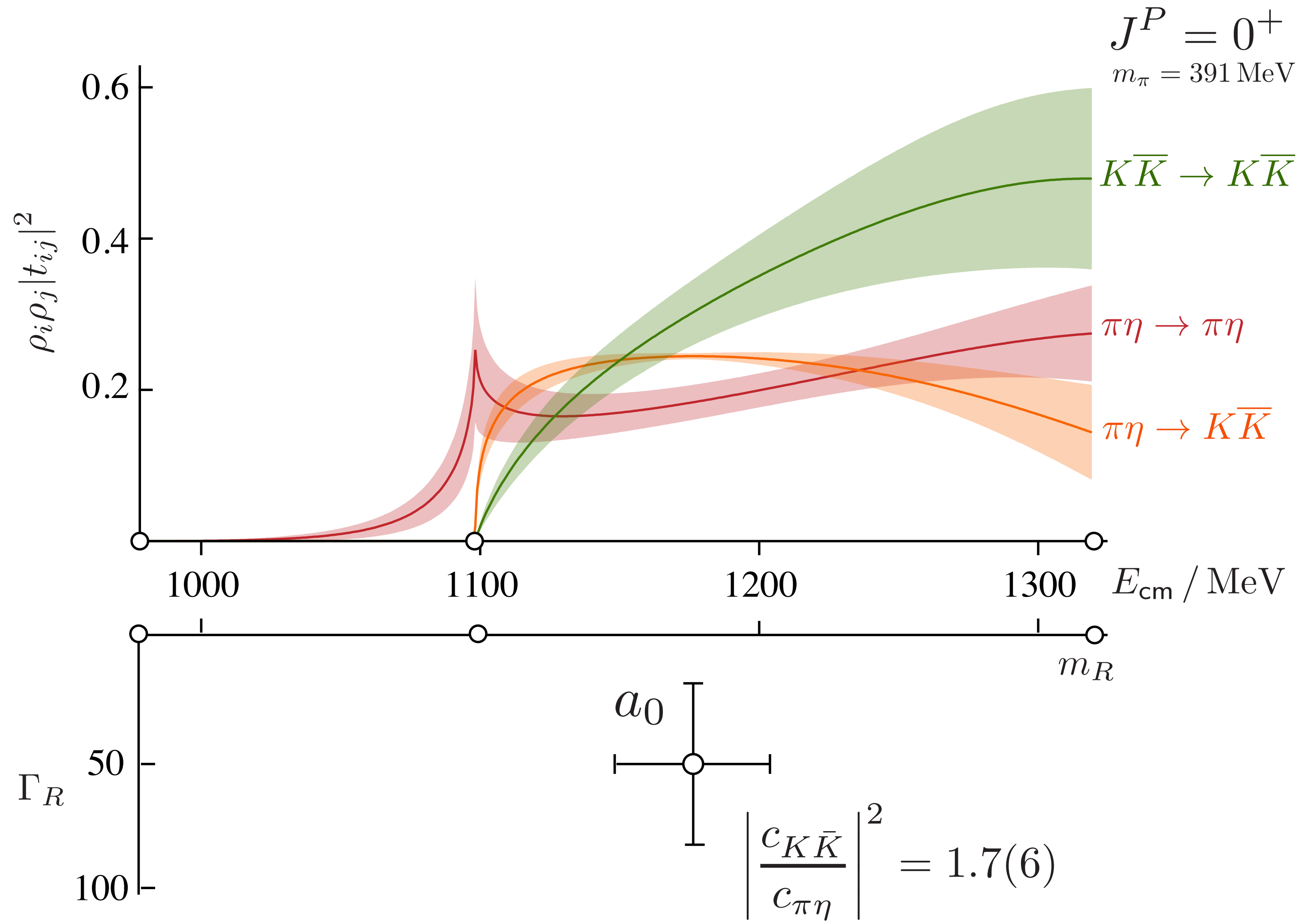


the $a_0$("980")

# $f_0$, $a_0$ similarities ?



masses similar

$$m_R(f_0) = 1166(45)\,\text{MeV},$$
$$m_R(a_0) = 1177(27)\,\text{MeV},$$

widths a little different

$$\Gamma_R(f_0) = 181(68)\,\text{MeV},$$
$$\Gamma_R(a_0) = 49(33)\,\text{MeV}.$$

but channel couplings quite similar ?

$$\left|c(a_0 \to K\overline{K})\right| \approx \left|c(f_0 \to K\overline{K})\right| \quad \sim 850\,\text{MeV}$$
$$\left|c(a_0 \to \pi\eta)\right| \approx \left|c(f_0 \to \pi\pi)\right| \quad \sim 700\,\text{MeV}.$$

main difference is the larger phase-space for $\pi\pi$ compared to $\pi\eta$

can explore the effect using the simple Flatté amplitude

Flatté denominator $D(s) = m_0^2 - s - i g_1^2\, \rho_1(s) - i g_2^2\, \rho_2(s)$

has zeros at

$$\sqrt{s_0} \approx m_0 \pm \frac{i}{2}\frac{g_2^2\,\rho_2}{m_0}\left[\left(\frac{g_1}{g_2}\right)^2 \frac{\rho_1}{\rho_2} - 1\right] \quad \text{on sheet II, if } \left(\frac{g_1}{g_2}\right)^2 \frac{\rho_1}{\rho_2} > 1, \text{ or,}$$

$$\sqrt{s_0} \approx m_0 \pm \frac{i}{2}\frac{g_2^2\,\rho_2}{m_0}\left[1 - \left(\frac{g_1}{g_2}\right)^2 \frac{\rho_1}{\rho_2}\right] \quad \text{on sheet IV, if } \left(\frac{g_1}{g_2}\right)^2 \frac{\rho_1}{\rho_2} < 1, \text{ and,}$$

$$\sqrt{s_0} \approx m_0 \pm \frac{i}{2}\frac{g_2^2\,\rho_2}{m_0}\left[1 + \left(\frac{g_1}{g_2}\right)^2 \frac{\rho_1}{\rho_2}\right] \quad \text{on sheet III, in all cases,}$$

# $\pi\pi$, $K\bar{K}$, $\eta\eta$ scattering with $m_\pi$~391 MeV

PRD 97 054513 (2018)



## *D*-wave amplitudes

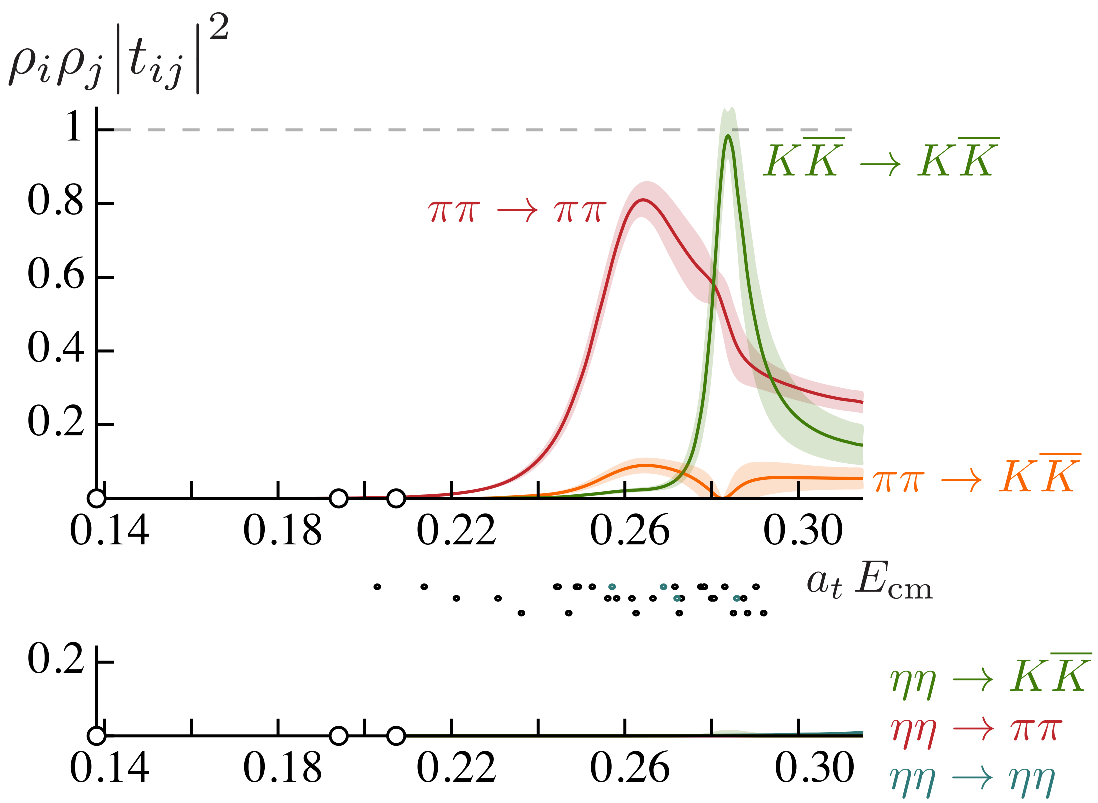


bumps are in the three channel region ⇒ **8 sheets !**

won't burden you with the sheet details here …

# $\pi\pi$, $K\bar{K}$, $\eta\eta$ scattering with $m_\pi$~391 MeV

PRD 97 054513 (2018)

*D*-wave amplitudes

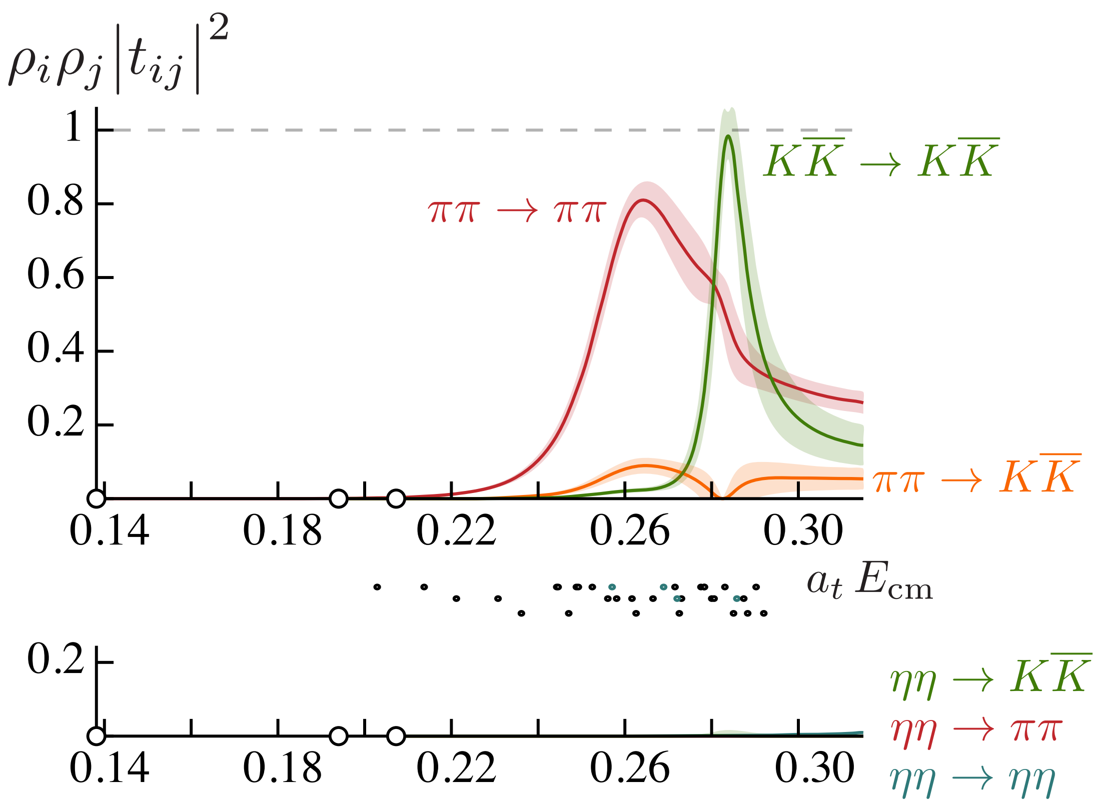


bumps are in the three channel region ⇒ **9 sheets !**

won't burden you with the sheet details here …

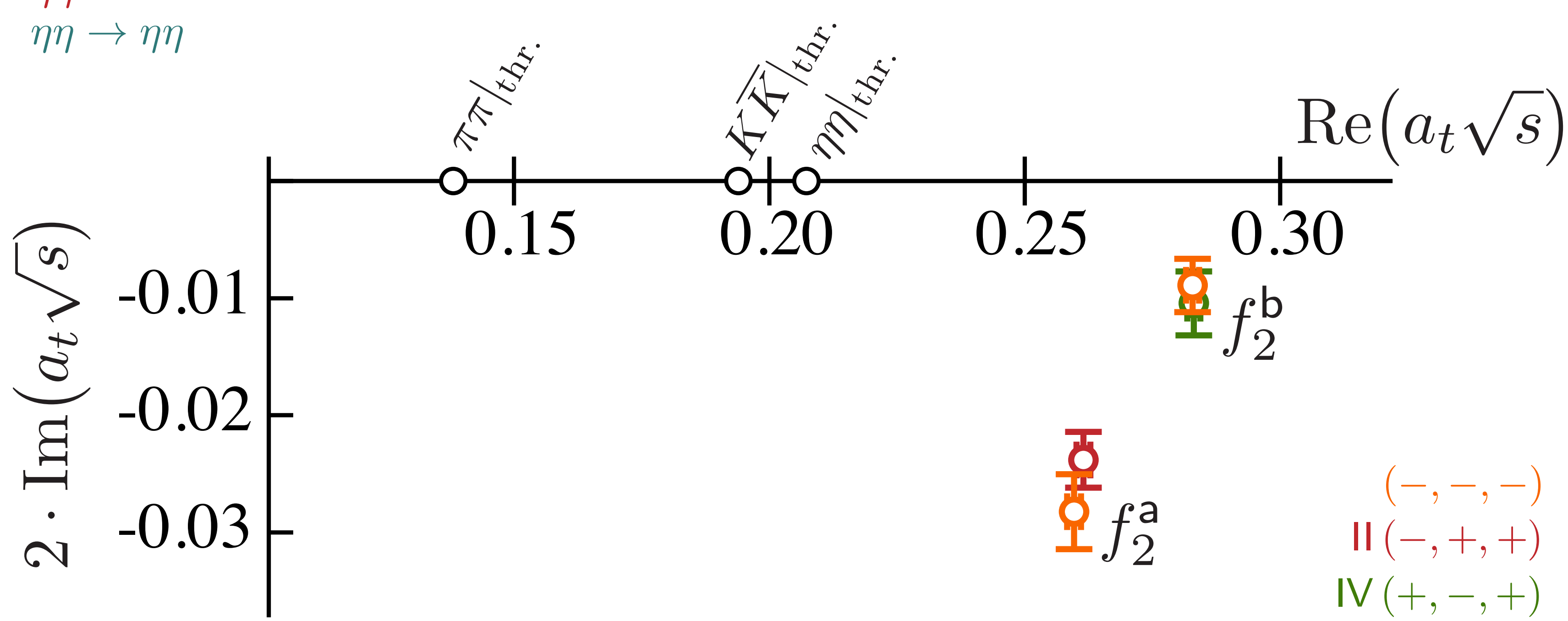


(–,–,–) is 'closest' sheet to physical scattering above all three thresholds

# couplings at the poles

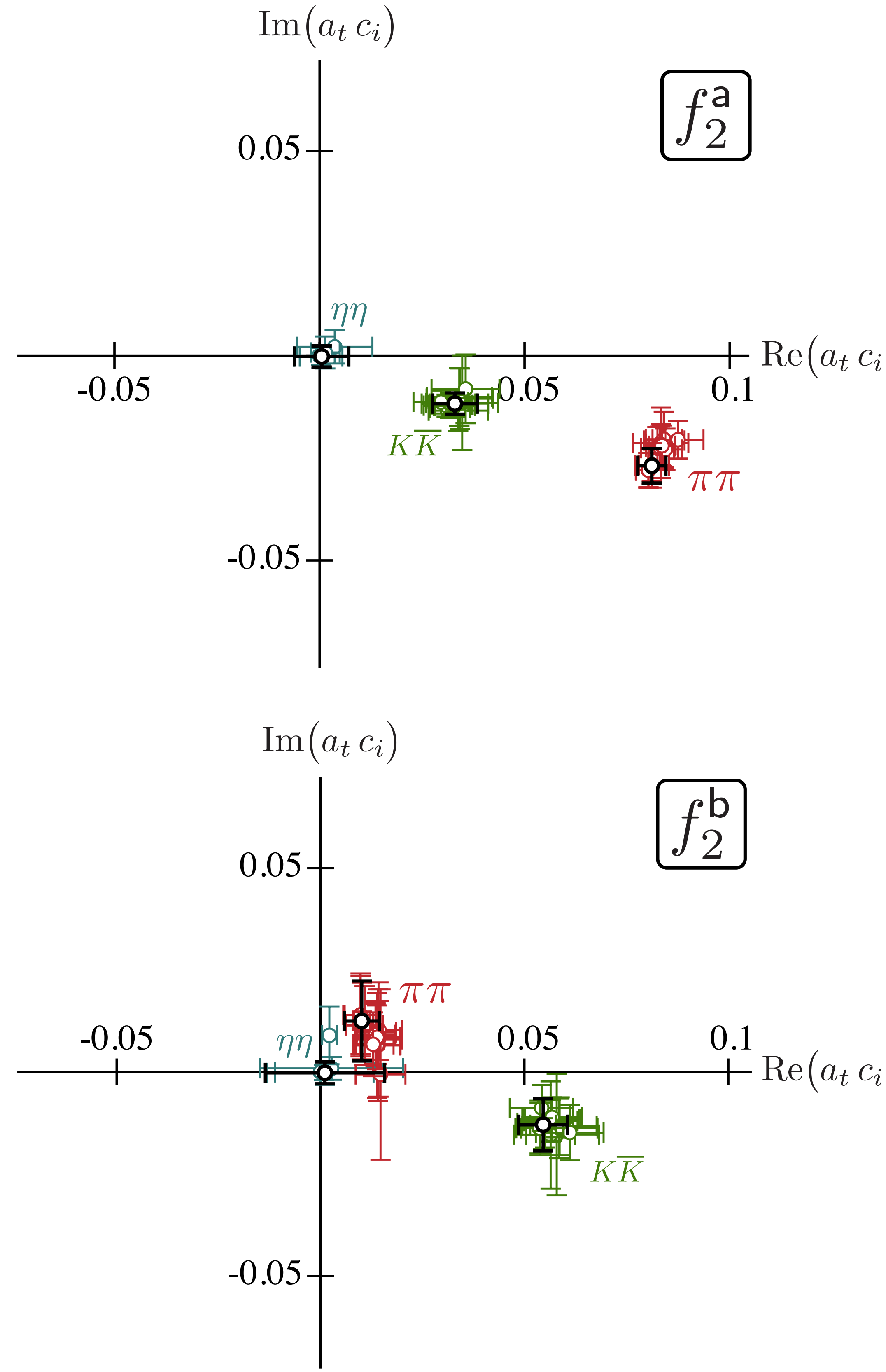

# $\pi\pi$, $K\bar{K}$, $\eta\eta$ scattering with $m_\pi$~391 MeV

## *D*-wave amplitudes & poles

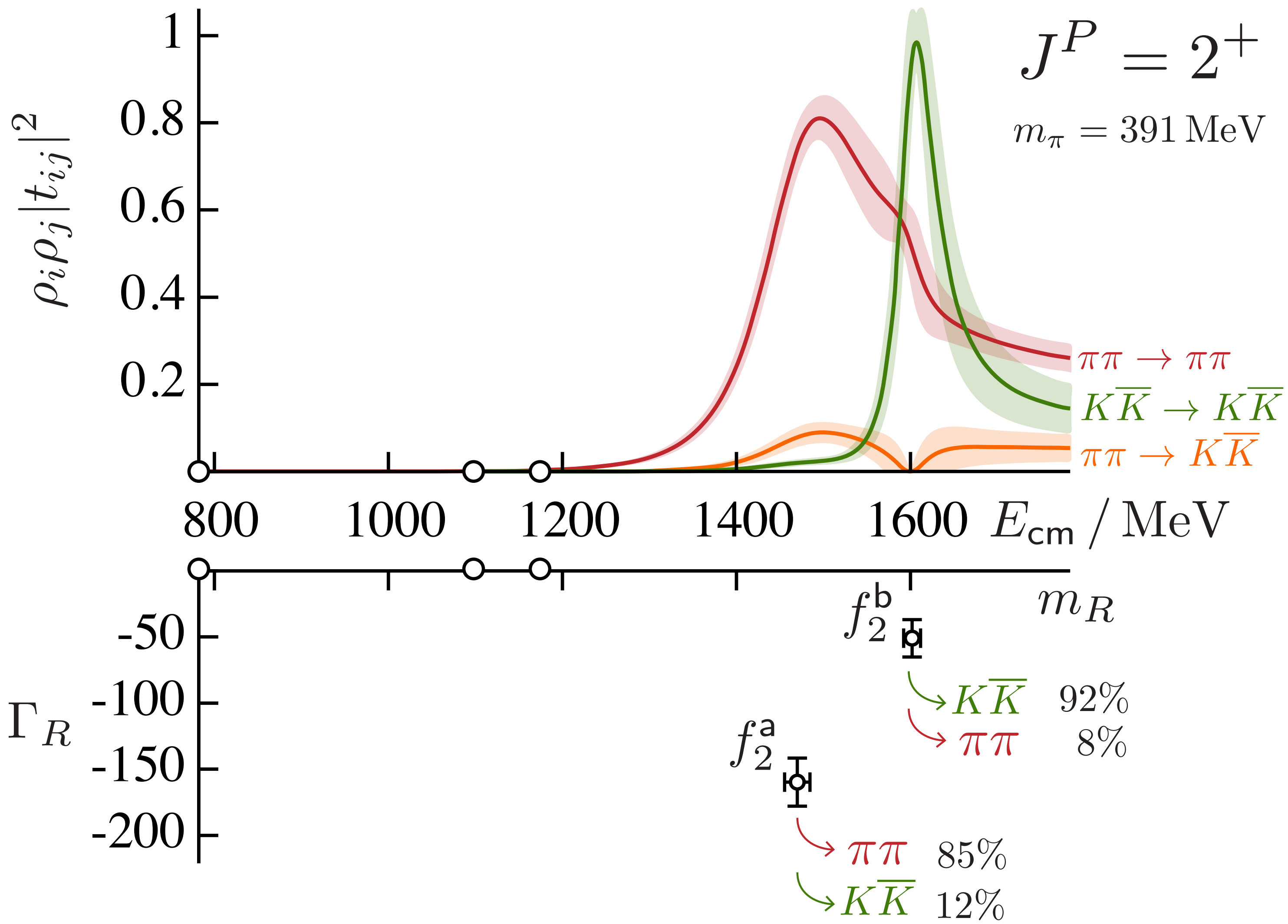


## pdg summary

**$f_2(1270)$** $I^G(J^{PC}) = 0^+(2^{++})$

Mass $m = 1275.5 \pm 0.8$ MeV
Full width $\Gamma = 186.7^{+2.2}_{-2.5}$ MeV (S = 1.4)

| $f_2(1270)$ DECAY MODES | Fraction ($\Gamma_i/\Gamma$) | Scale factor/ Confidence level | $p$ (MeV/c) |
|---|---|---|---|
| $\pi\pi$ | $(84.2\ ^{+2.9}_{-0.9})$ % | S=1.1 | 623 |
| $\pi^+\pi^-2\pi^0$ | $(7.7\ ^{+1.1}_{-3.2})$ % | S=1.2 | 563 |
| $K\bar{K}$ | $(4.6\ ^{+0.5}_{-0.4})$ % | S=2.7 | 404 |
| $2\pi^+2\pi^-$ | $(2.8\ \pm 0.4)$ % | S=1.2 | 560 |
| $\eta\eta$ | $(4.0\ \pm 0.8) \times 10^{-3}$ | S=2.1 | 326 |
| $4\pi^0$ | $(3.0\ \pm 1.0) \times 10^{-3}$ | | 565 |

**$f_2'(1525)$** $I^G(J^{PC}) = 0^+(2^{++})$

Mass $m = 1525 \pm 5$ MeV [l]
Full width $\Gamma = 73^{+6}_{-5}$ MeV [l]

| $f_2'(1525)$ DECAY MODES | Fraction ($\Gamma_i/\Gamma$) | $p$ (MeV/c) |
|---|---|---|
| $K\bar{K}$ | $(88.7\ \pm 2.2)$ % | 581 |
| $\eta\eta$ | $(10.4\ \pm 2.2)$ % | 530 |
| $\pi\pi$ | $(8.2\ \pm 1.5) \times 10^{-3}$ | 750 |

**left-hand cuts** are effect of scattering in **crossed-channels**

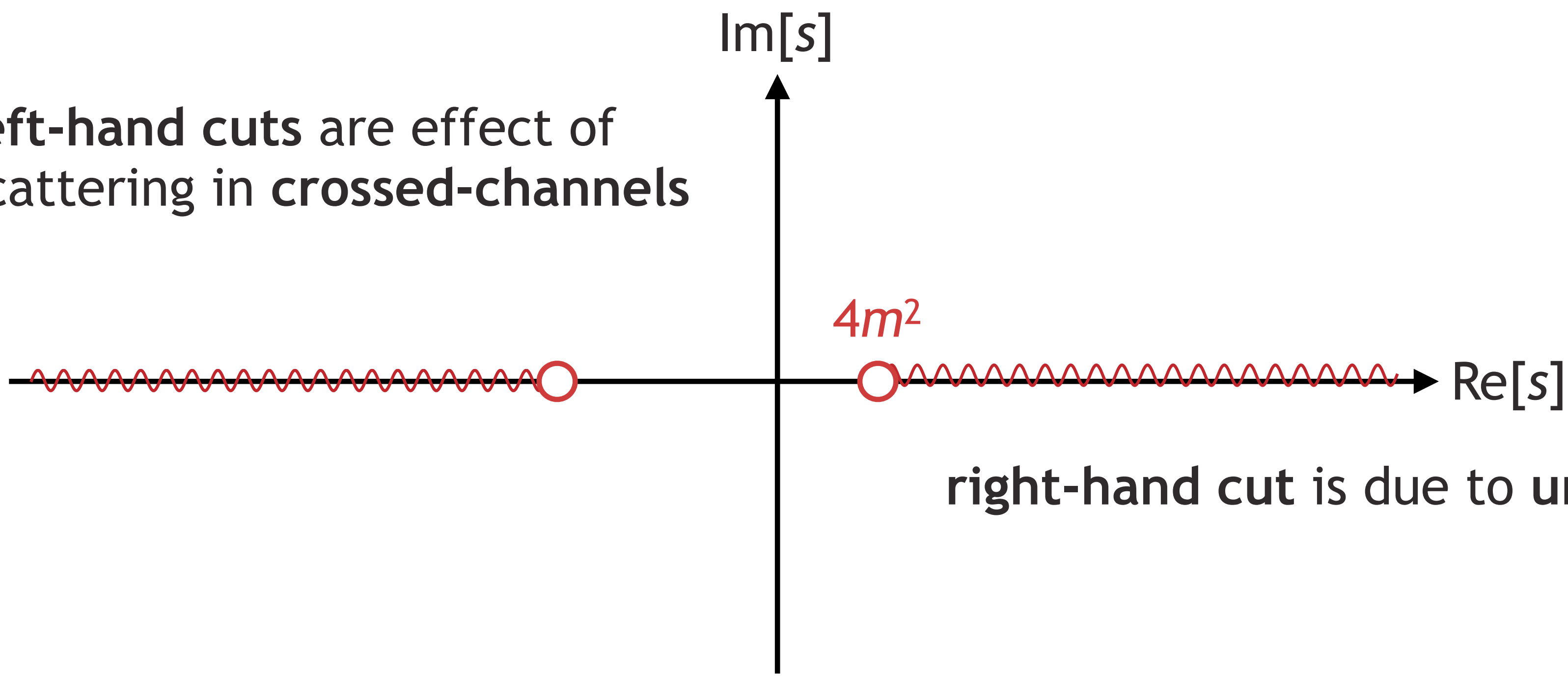


**right-hand cut** is due to **unitarity**

a very simple-minded toy model illustrating a left-hand cut:

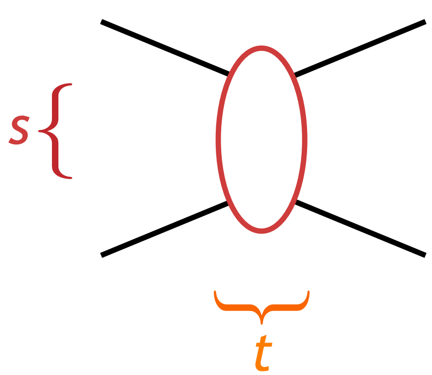


$$t = -2k^2(1-\cos\theta)$$
$$s = 4(m^2+k^2)$$

suppose there is a $t$-channel stable meson exchange

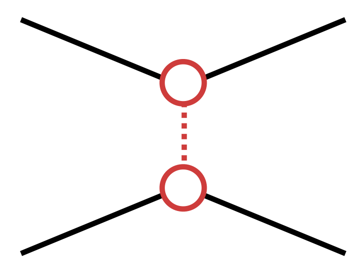

$$f(s,t) \sim \frac{1}{t-M^2}$$

S-wave partial-wave projection

$$t_\ell(s) \sim \int d\cos\theta \; f\big(s, t(\cos\theta)\big)$$
$$= -\frac{1}{2k^2}\log\left[s-(4m^2-M^2)\right]$$

log branch cut from $4m^2 - M^2$

**left-hand cuts** are effect of scattering in **crossed-channels**

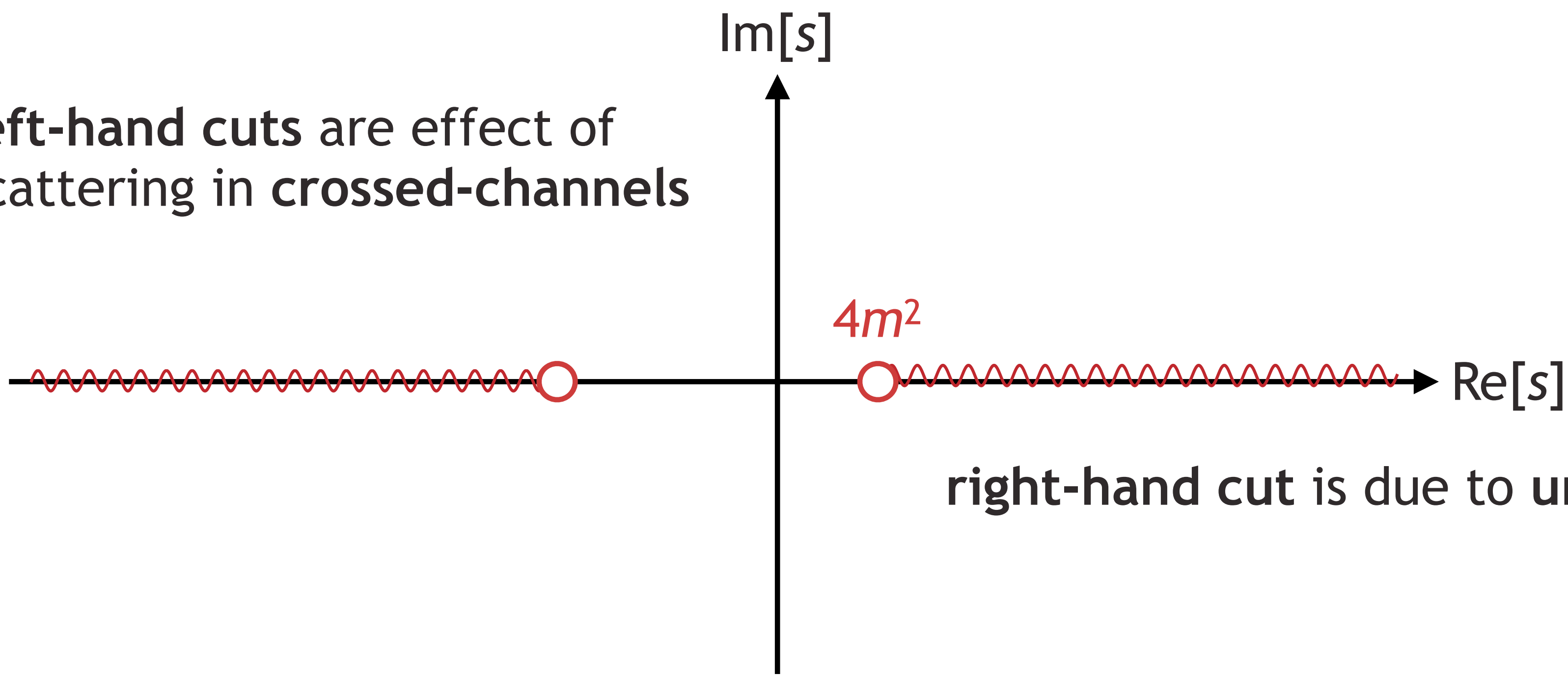


**right-hand cut** is due to **unitarity**

more generally **unitarity** in the $t$-channel
ensures there will be a left-hand cut in partial-wave amplitudes

# where left-hand cuts don't matter



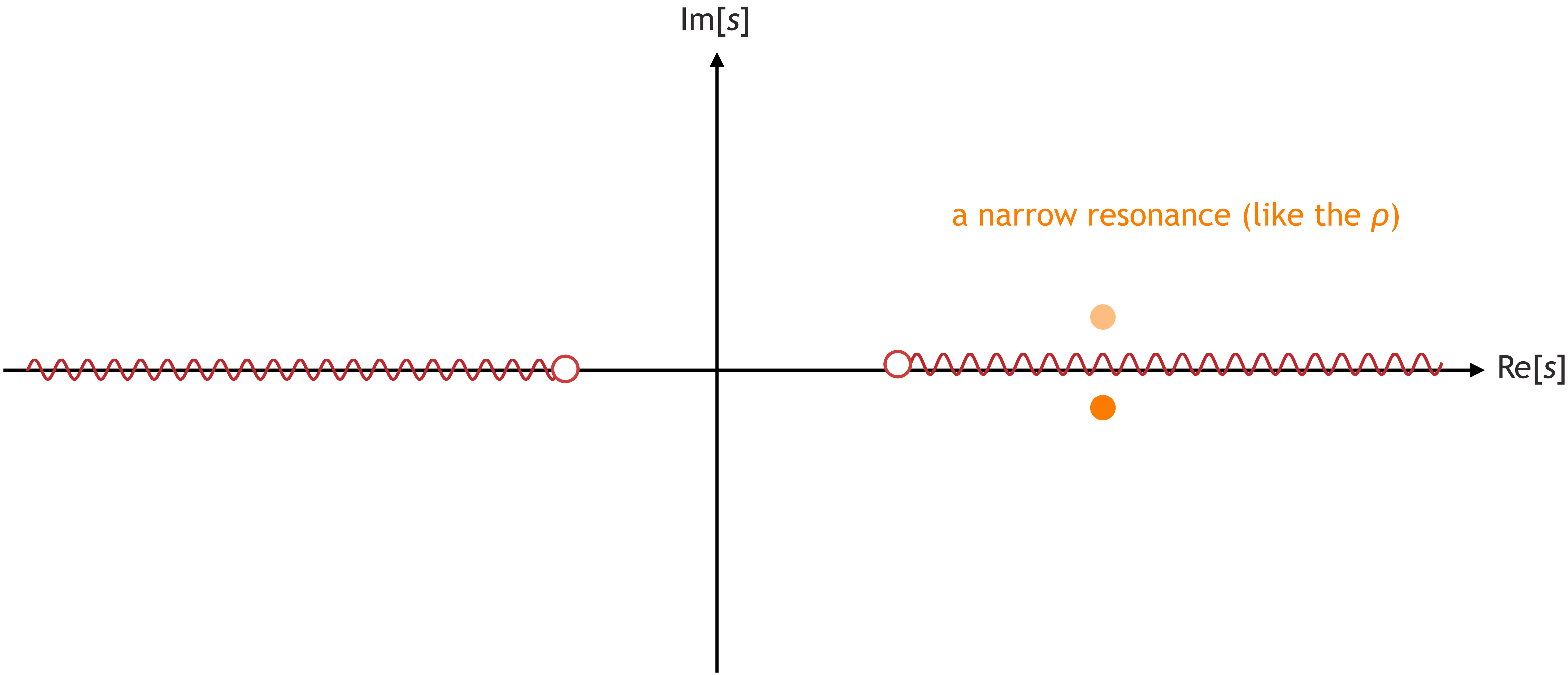

# where left-hand cuts don't matter



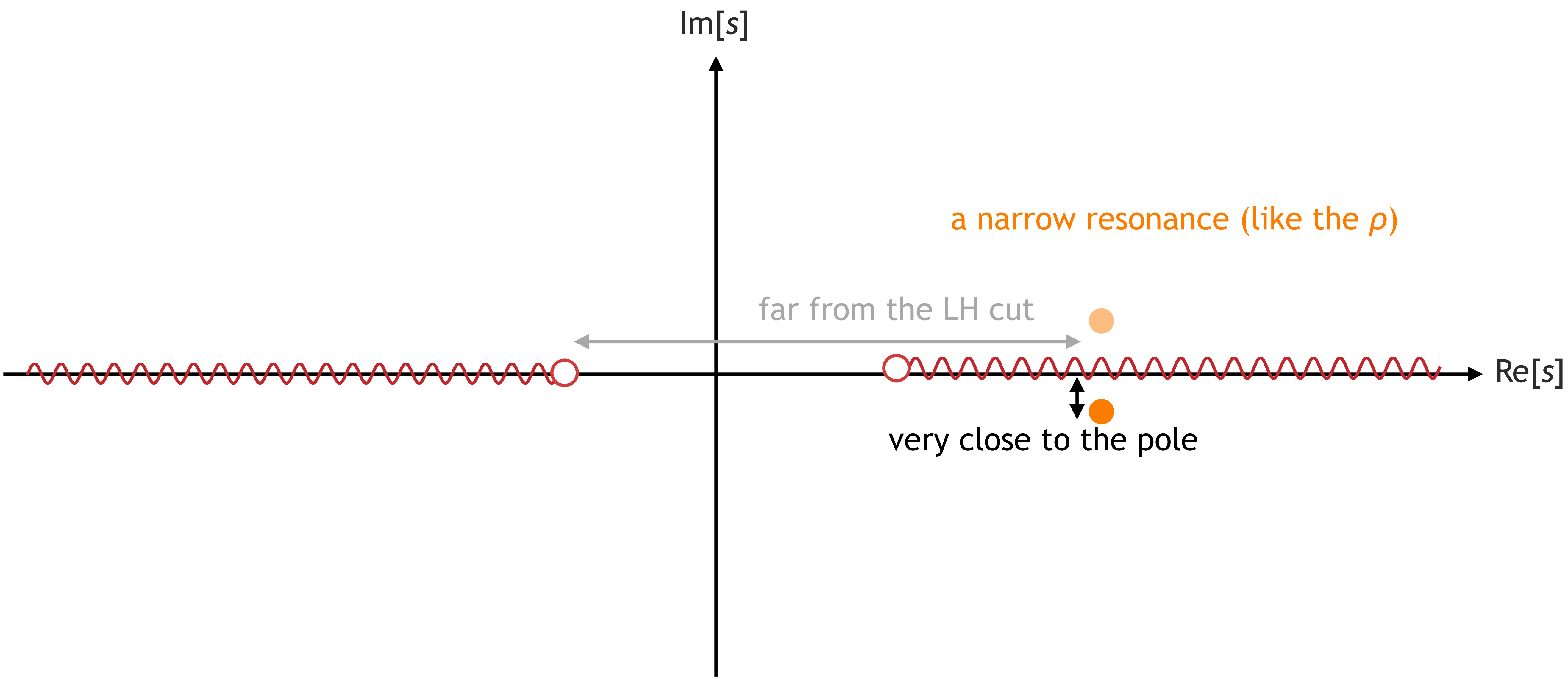

# where left-hand cuts matter (maybe ?)



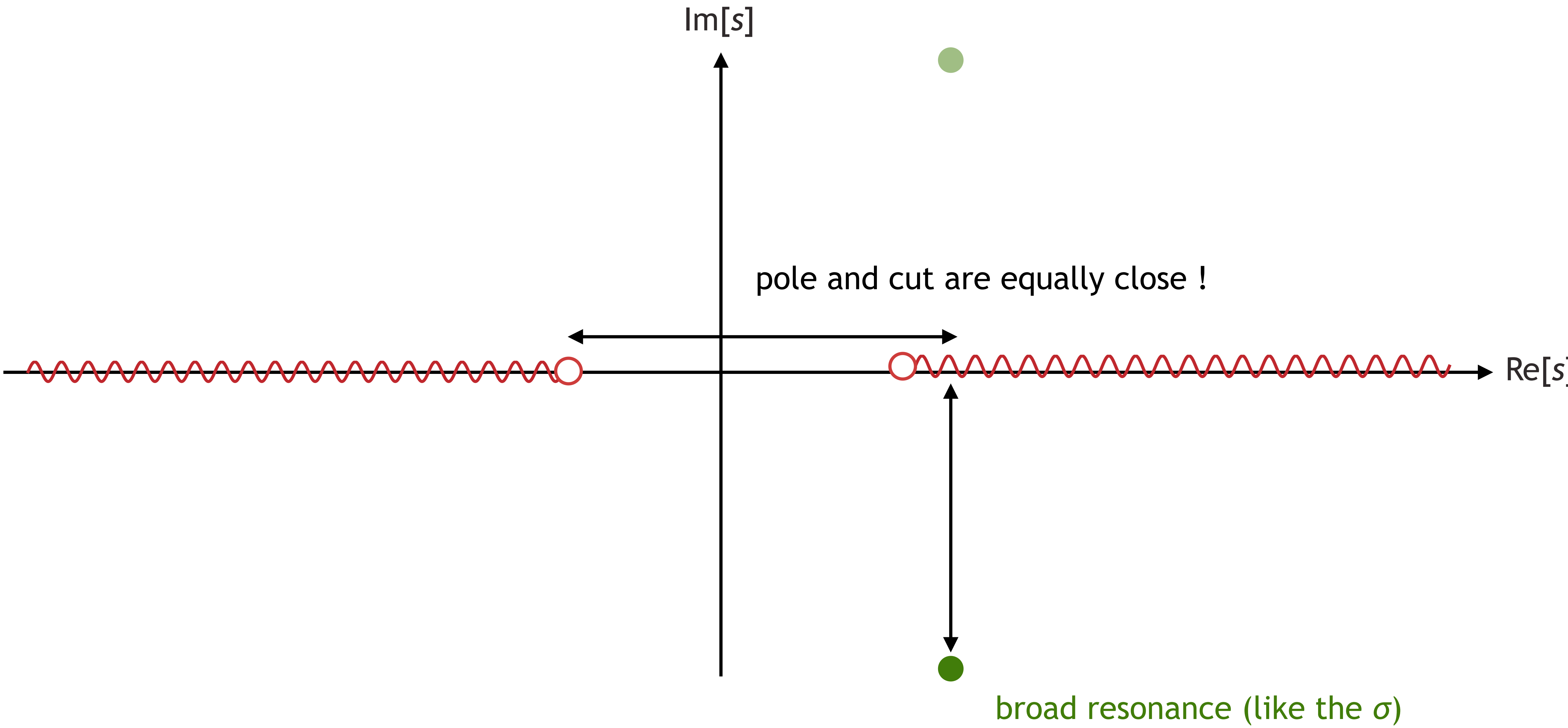

$\pi\pi$ isospin=0